

DEFORMATION OF AN ISLAND ARC:
 RATES OF MOMENT RELEASE AND CRUSTAL SHORTENING
 IN INTRAPLATE JAPAN DETERMINED FROM SEISMICITY AND QUATERNARY FAULT DATA

Steven G. Wesnousky and Christopher H. Scholz

Department of Geological Sciences and Lamont-Doherty Geological Observatory of Columbia University
 Palisades, New York 10964

Kunihiko Shimazaki

Earthquake Research Institute, University of Tokyo, Bunkyo-ku, Tokyo, Japan

Abstract. The historical record of large ($M > 6.9$) earthquakes and geologically determined rates of slip on Quaternary faults in intraplate Japan (Honshu and Shikoku) are used to estimate the average rate of seismic moment release (\dot{M}) for the last 400 years and during the late Quaternary, respectively. Values of \dot{M} estimated from the two data sets are similar in regions where seismic activity is concentrated on land. We interpret this observation to suggest that \dot{M} in intraplate Japan has been constant during the late Quaternary and is relatively free from secular variation when averaged over periods of several hundreds of years. \dot{M} in Shikoku may be attributed almost solely to right-lateral slip of the median tectonic line (MTL). The easterly strike of the MTL is consistent with a compressive stress field that trends northwest. Crustal shortening of the Izu Peninsula taken up on a set of strike slip faults that show north by northwest compression is ≈ 1 mm/yr. Northeast Honshu is characterized by a set of reverse-type faults that trend northerly. Conversion of \dot{M} in northeast Japan to strain rates suggests that about 5% of the relative plate motion between Japan and the Pacific plate (≈ 9.7 cm/yr) is accommodated as a permanent east-west shortening (≈ 5 mm/yr) of northeast Honshu. The predominant deformation in central and western Honshu takes place as slip on a conjugate system of strike slip faults that strike northeast and southeast and show right-lateral and left-lateral motion, respectively. Crustal shortening, resulting from slip on faults, in central and western Honshu is 5 and 0.5 mm/yr, respectively, in an easterly direction. Central and western Honshu are in closest proximity to the Nankai trough, and hence, the stress field in these regions cannot simply be attributed to the accommodation of the relative (northwesterly) convergence of the Philippine Sea plate. The northward impingement of the Izu Peninsula into Honshu may influence stresses in central and western Japan, but a conclusive explanation of the stress field in central and western Honshu remains an enigma.

Introduction

The common occurrence of intraplate seismicity and mountain belts adjacent to convergent plate boundaries indicates that a significant portion

of relative plate motion takes place as a permanent strain of the overriding plate. In this study, seismicity and Quaternary fault data are used to quantify the amount of horizontal deformation that results from slip on faults within the crust of the islands of Honshu and Shikoku, part of the Japanese island arc system. It is for this region that by far the most complete set of data concerning seismicity and Quaternary faulting is available.

The seismic moment tensor (\tilde{M}) is the most direct measure of the elastic waves set up by an earthquake and the deformation resulting from its occurrence [e.g., Aki, 1966; Aki and Richards, 1980]. For shearing on a fault, the scalar value of the seismic moment (M_0) is $\mu A u$, where μ is the shear modulus, u is the average slip on the fault, and A is the fault area. The moment tensor (\tilde{M}) can be completely described when the strike, dip, and rake of the fault are known in addition to M_0 . In this study, the seismic moments of large intraplate earthquakes ($M > 6.9$) in Japan are gathered from the literature or, in the case of historical earthquakes, determined from intensity data. Kostrov's [1974] formula relating seismic moment to strain is then used to calculate the amount of strain that has resulted from slip during earthquakes over the last 400 years. Similar to earthquakes, active Quaternary faults with geologically estimated slip rates are described in terms of their average rate of seismic moment release and utilized to determine the average rates of strain of Japan during the late Quaternary period. The values obtained for the different periods of time are then used as the basis for deciding whether or not the rate of fault deformation in intraplate Japan has been constant during the Quaternary period.

Plate Tectonic Setting and Seismicity of Japan

The Japanese island arc is located along the eastern border of the Eurasian plate and bounded to the east and south by the Pacific and Philippine Sea plates, respectively (Figure 1). The majority of earthquakes in Japan, including the largest ($M_0 > 10^{28}$ dyne cm), occur along the Japan trench and the Sagami and Nankai troughs [e.g., Usami, 1966, 1975]. Focal mechanisms of large earthquakes along these features are usually of the low-angle thrust type and interpreted to indicate that the Pacific and Philippine Sea plates are being subducted beneath northeastern and southwestern Japan, respectively [Fitch and Scholz, 1971; Kanamori, 1971, 1972; Ando, 1974b, 1975; Abe, 1977; Scholz and Kato, 1978].

Copyright 1982 by the American Geophysical Union.

Paper number 2B0732.
 0148-0227/82/002B-0732\$05.00

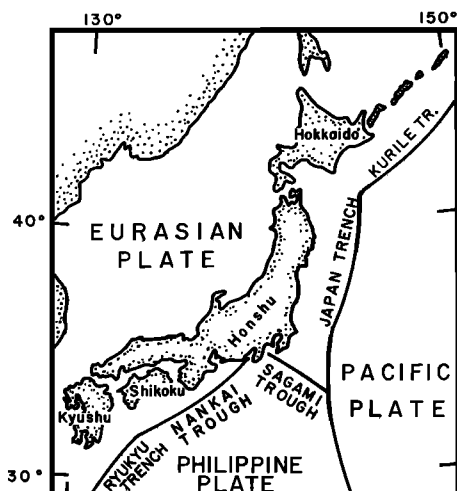


Fig. 1. Regional plate tectonic setting.

Yamashina et al. [1978] studied shallow seismicity in Japan and other island arcs and defined a zone extending along the frontal non volcanic arc, characterized by a very low rate of seismicity, as the 'aseismic belt.' The shallow seismicity landward of the aseismic belt is referred to here as intraplate seismicity and generally does not extend to depths greater than 15 km [e.g., Oike, 1975; Takagi et al., 1977; Watanabe et al., 1978] (Figure 2). The seismic moments of the largest intraplate earthquakes are about 10^{27} dyne cm, an order of magnitude or more less than seismic moments of the great interplate earthquakes.

Focal mechanism data have been used to delineate the ambient intraplate stress field in Japan [e.g., Honda, 1932; Honda and Masatsuka, 1952; Honda et al., 1956, 1967; Ichikawa, 1970, 1971; Nishimura, 1973; Yamashina, 1976; Shiono, 1977]. A summary of 44 intraplate events with magnitudes of about 6.0 and greater is presented in Table 1. Fault mechanisms of intraplate earthquakes are usually strike slip or high-angle reverse, and the distribution of P axes reveals that Honshu is, in general, subject to a regional maximum compressive stress that trends easterly (Figure 3). Normal faulting is found in Kyushu, adjacent to the junction of the Nankai Trough and Ryukyu Trench. Near the junction of two arc systems, the state of stress within the earth's crust generally differs from the regional trend [Shimazaki et al., 1978]. Hokkaido, like Kyushu, is also located near the junction of two trenches (Figure 1). We limit the remainder of this study to the islands of Honshu and Shikoku, adjacent to the Japan trench and the Nankai and Sagami troughs. For convenience, we will refer to this region as intraplate Japan.

The P axes of intraplate earthquakes in Honshu are approximately aligned with the relative plate velocity vector along the Japan trench (Figure 3). This alignment has been interpreted to arise from the transmission of compressive stress across the Japan trench [e.g., Ichikawa, 1971; Shiono, 1977; Nakamura and Uyeda, 1980]. Focal mechanisms differ between northeast Honshu and regions to the southwest (Figure 3). Earthquakes in northeastern Honshu commonly are high-angle

reverse on planes that strike north. Earthquakes in central and western Honshu generally exhibit strike slip movement of a left- or right-lateral nature on northwest or northeast striking fault planes, respectively. The area in and adjacent to the Izu Peninsula, at the junction of the Sagami and Nankai troughs, is also marked by strike slip faulting but in contrast to the remainder of Honshu, the P axes trend to the north. The Izu Peninsula appears to be a part of the Philippine Sea plate, and the northerly trend of P axes in this area is probably a manifestation of the recent collision of the Izu Peninsula with Honshu [Matsuda, 1978; Somerville, 1978]. The seismicity in this region also differs from the remainder of intraplate Japan in that it is not landward of a trench.

Quaternary Faulting

The orientation and displacement of Quaternary faults closely mimics movement observed in recent earthquakes (Figure 4) [Research Group for Active Faults of Japan, 1980a, b]. Quaternary faults in northeastern Honshu are of the reverse type, strike northerly, and are distributed relatively uniformly through the region. The concentration of Quaternary faulting is greatest in central Honshu. The predominant deformation in central Honshu takes place as slip on a conjugate system of strike slip faults that strike northeast and northwest and show right- and left-lateral motion, respectively. This same motion of faulting is also seen in western Honshu, where the density of faulting is much less. Faults in the Izu Peninsula region are also strike slip but are consistent with a compressive stress that trends north to northwest [Somerville, 1978]. Hence,

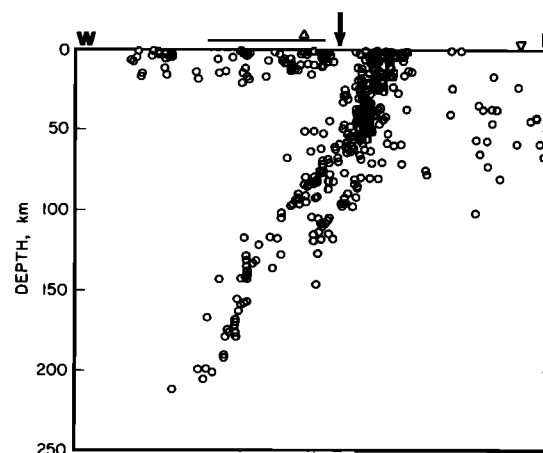


Fig. 2. Focal depth distribution of microearthquakes projected on an east-west cross section (adapted from Hasegawa et al. [1978]). Seismicity from 38° - 39° N is plotted. Arrow indicates approximate location of the 'aseismic belt' [Yamashina et al., 1978]. Triangle and reverse triangle represent positions of volcanic front and Japan trench, respectively. Location of Japanese Islands is delineated by horizontal line above cross section. Intraplate seismicity is located in upper 15 km of crust, west of the aseismic belt. The figure has a vertical exaggeration of 2.

intraplate deformation in Honshu takes place as slip on a network of faults that accommodate a regional compressive stress field that trends east except for the Izu Peninsula, where maximum horizontal stress is oriented north to northwest.

Strain release in Shikoku occurs by slip along the median tectonic line (MTL), a major right-lateral fault that strikes easterly, across the northern coast of Shikoku and parallel to the Nankai trough (Figure 3). The orientation and slip of the MTL is consistent with a compressive stress that trends northwest, in contrast to an easterly maximum compression in Honshu. In summary, geologic and seismologic data may be used to divide intraplate Japan into five regions of distinct tectonic style: (1) northeast Honshu, (2) central Honshu, (3) western Honshu, (4) Shikoku, and (5) the Izu Peninsula and adjacent environs (Figure 5).

The Seismic Moment Tensor

The seismic moment tensor for a hypothetical shear dislocation at a point may be expressed as

$$\tilde{M} = M_0(b_1n_j + b_jn_i) \quad (1)$$

where M_0 is the scalar value of the moment and b and n are unit vectors in the direction of slip and normal to the fault plane, respectively. The P , T , and B axes of focal mechanism solutions correspond to the principal axes of the moment tensor [e.g., Aki and Richards, 1980]. Brune [1968] showed that the slip rate along a fault may be expressed in terms of the seismic moment as

$$\dot{u} = \frac{1}{\mu ST} (\Sigma M_0) \quad (2)$$

where \dot{u} is the average slip rate, μ shear modulus, S surface area of fault plane, T time period over which seismicity occurred, and ΣM_0 the cumulative sum of moments of all earthquakes occurring on the fault area S over time T .

Brune [1968] and Davies and Brune [1971] used (2) to calculate average slip rates along major plate boundaries, using a record of seismicity extending back as little as 50 years. Their ability to do this was contingent on the high slip rates (cm/yr) and short recurrence times (tens to hundreds of years) of large earthquakes along given segments of plate boundaries. The style of seismicity within intraplate Japan is distinctively different. Slip rates along given faults are less (mm/yr), recurrence times greater (several hundreds to thousands of years), and seismic energy release is not concentrated along one fault but rather is divided among a large network of faults (Figures 4 and 5). Hence, in a region like this it is not appropriate to consider only a single fault. It is more suitable to measure the total deformation resulting from the movements on all faults in the area. Kostrov [1974] expanded the method proposed by Brune [1968] to determine the average strain of a region where seismicity is distributed uniformly in a volume rather than restricted to a given fault.

The mean rate of strain ($\dot{\epsilon}$) of a seismogenic volume (V) resulting from earthquake dislocations is proportional to the sum of the seismic moment tensors ($\Sigma \tilde{M}$) of all earthquakes occurring in the volume (V) per unit time (T) [Kostrov, 1974]:

$$\dot{\epsilon} = \frac{1}{2\mu VT} (\Sigma \tilde{M}) \quad (3)$$

Cumulative offsets on geologic faults may be assumed as the sum of displacements resulting from many earthquakes. Hence, the average rate of slip of a geologic fault may be used to estimate the average rate of moment release of the fault. We use formula (3) plus seismicity and Quaternary fault data to analyze crustal deformation in intraplate Japan.

Deformation Rates From Seismicity Data

Data

In this work, data for earthquakes prior to 1885 are from the 'Descriptive Catalogue of Disastrous Earthquakes in Japan' [Usami, 1975]. Data from Utsu's [1979] catalogue is used for the period 1885-1925. Magnitudes and epicentral data for events after 1925 are acquired from the Supplementary *Seismological Bulletin* of the Japan Meteorological Agency (JMA) [1958, 1966, 1968] (and monthly bulletins thereafter). Magnitudes in each catalogue are scaled to conform with the definition of surface wave magnitude proposed by Gutenberg and Richter [1954].

Most of the cumulative deformation resulting from seismicity occurs during the largest earthquakes [Brune, 1968]. We thus limit our concern to large earthquakes, defined here as those events with magnitudes greater than or equal to 6.9 (or $M_0 \approx 10^{26}$ dyne cm). A plot of large intraplate earthquakes versus time for the last 400 years shows that the frequency of occurrence of large events has been higher for the period since 1880 than for the prior 300 years (Figure 6c). The greater frequency of events observed for the last 100 years reflects the initiation of both instrumental recording [Kikuchi, 1904] in 1880 and the systematic collection of felt reports by the Central Meteorological Observatory in 1884 [Usami and Hamamatsu, 1967]. Prior to this time, even though since the commencement of the 17th century it has been 'the rule of the government to have each feudal chief send in a detailed report of damage caused in his dominion by an earthquake or other natural events' [Omori, 1899], it appears that a number of even the large events may be missing from the historical record. The spatial distribution of seismicity discloses those areas that are deforming most intensely. It is thus important to investigate whether data possibly missing from the earlier period (1581-1880) may account for any spatial distortion in the observed pattern of seismicity.

The epicentral distributions of large earthquakes during the periods 1581-1880 and 1881-1980 are compared in Figure 5. Two major differences are immediately evident in the pattern of seismicity in the two periods. The first is the absence of seismicity on the Izu Peninsula during the earlier period as compared to the occurrence

TABLE 1. Events With Magnitude of About 6.0 and Greater for Which Focal Mechanism Has Been Determined

Earthquake Data*										Focal Mechanism Data			
No.	Location	Date	Magnitude	Latitude Longitude		Depth km	Reference	P Axis		T Axis		Reference	
				°N	°N			Trend	Plunge	Trend	Plunge		
1	Tango	March 7, 1927	7.75 [†]	35.6	135.1	10	JMA	110	0	20	0	Honda [1932]	
2	N. Izu	Nov. 26, 1930	7.0	35.1	139.0	~5	JMA	144	0	54	0	Honda [1931] and Abe [1978]	
3	Chugoku Mts.	Dec. 20, 1930	7.0	35.0	132.9	20	JMA	97	0	187	0	Ichikawa [1971]	
4	Yamanashi	Sept. 16, 1931	6.5	35.5	138.9	35	JMA	207	29	55	58	Shiono [1977]	
5	Saitama	Sept. 21, 1931	7.0	36.1	139.2	~15	JMA	55	0	145	0	Ichikawa [1971]	
6	S. Izu	March 21, 1934	5.5	34.8	138.9	~5	JMA	172	10	127	0	Abe [1978]	
7	Gifu	Aug. 18, 1934	6.2	35.7	137.0	~5	JMA	95	0	5	0	Ichikawa [1971]	
8	Shizuoka	July 11, 1935	6.3	35.0	138.4	10	JMA	26	0	116	0	Ichikawa [1971]	
9	Osaka	Feb. 21, 1936	6.4	34.5	135.7	20	JMA	266	19	161	35	Shiono [1977]	
9a	Ogahanto	Jan. 14, 1939	7.0	40.0	139.8	0	JMA	283	26	155	52	Yamashina [1976]	
10	Off Shakotan	Aug. 1, 1940	7.0	44.4	139.5	~33	Fukao and Furumoto [1975]	260	1	355	80	Fukao and Furumoto [1975]	
11	Near Oki Is.	Aug. 14, 1940	6.8	36.2	132.2	~15	JMA	96	14	358	28	Shiono [1977]	
12	Near Nagano	July 15, 1941	6.2	36.7	138.3	~10	JMA	86	0	176	0	Ichikawa [1971]	
12a	Near Nagano	Aug. 12, 1943	6.1	37.3	139.8	15	JMA	245	~4	135	77	Yamashina [1976]	
13	Tottori	Sept. 10, 1943	7.4	35.5	134.2	10	JMA	116	0	26	0	Ichikawa [1971]	
14	Near Nagano	Oct. 13, 1943	6.1	36.8	138.2	0	JMA	142	0	26	0	Ichikawa [1971]	
15	Mikawa	Jan. 13, 1945	7.1	34.8	137.1	5	Ando [1974a]	71	18	212	68	Ando [1974a]	
16	Fukui	June 28, 1948	7.3	36.1	136.2	20	JMA	125	0	35	0	Ichikawa [1971]	
17	N. Hyogo	Jan. 20, 1949	6.5	35.6	134.6	20	JMA	135	0	45	0	Ichikawa [1971]	
18	Imaichi	Dec. 25, 1949	6.7	36.7	139.7	~10	JMA	101	6	3	54	Yamashina [1976]	
19	Daishoji	March 7, 1952	6.8	36.5	136.2	20	JMA	122	0	32	0	Ichikawa [1971]	
20	S. Tokushima	July 27, 1955	6.0	33.8	134.3	~10	JMA	81	0	171	0	Ichikawa [1971]	

20a	Futatsui	Oct. 19, 1955	5.7	40.3	140.2	0	JMA	113	10	300	75	Yamashina [1976]
21	Shiroishi	Sept. 29, 1956	6.1	38.0	140.5	20	JMA	90	15	270	75	Yamashina [1976]
22	Near Miyakejima	Dec. 21, 1956	6.0	33.8	139.6	20	JMA	122	6	216	37	Maki [1974]
23	Near Niijima	Nov. 10, 1957	6.0	34.3	139.4	0	JMA	107	8	200	20	Yamashina [1976]
24	Teshikaga	Jan. 30, 1959	6.2	43.4	144.4	20	JMA	112	0	22	0	Ichikawa [1971]
25	Kita-Mino	Aug. 19, 1961	7.0	36.1	136.8	2	Kawasaki [1975]	270	8	164	63	Kawasaki [1975]
26	Kita-Miyagi	April 30, 1962	6.5	38.7	141.1	0	JMA	257	4	153	75	Yamashina [1976]
27	Wakasa Bay	March 26, 1963	6.9	35.8	135.8	4	Abe [1974]	283	1	14	31	Abe [1974]
28	Off Oga Penin.	May 7, 1964	6.9	40.4	139.0	22	ISC	121	5	301	85	Fukao and Furumoto [1975]
29	Niigata	June 16, 1964	7.5	38.4	139.3	12	Abe [1975b]	279	11	99	79	Abe [1975b]
30	Shizuoka	April 19, 1965	6.1	34.9	138.3	20	JMA	179	17	278	28	Maki [1974]
31	Ebino	Feb. 21, 1968	6.1	32.0	130.7	0	JMA	227	22	135	6	Yamashina [1976]
32	Gifu	Sept. 9, 1969	6.6	35.8	137.1	0	JMA	108	0	18	0	JMA
33	Akita	Oct. 16, 1970	6.2	39.2	140.7	6	JMA	44	0	134	74	Hasegawa et al. [1974]
34	Off Atsumi Pen.	Jan. 4, 1971	6.1	34.6	137.1	27	Oida and Ito [1972]	155	10	67	8	Oida and Ito [1972]
35	Fukui-Gifu	Aug. 31, 1972	6.0	35.9	136.8	10	JMA	270	3	5	59	Yamashina [1976]
36	Izu-Hanto-Okii	May 8, 1974	6.9	34.6	138.8	10	Abe [1978]	169	20	78	0	Abe [1978]
37	Amagi	July 9, 1974	4.9	34.8	138.9	~3	Abe [1978]	168	15	266	17	Abe [1978]
38	N. Aso	Jan. 23, 1975	6.1	33.0	131.1	0	JMA	90	54	352	6	Yamashina and Murai [1975]
39	Oita	April 20, 1975	6.4	33.2	131.2	0	JMA	86	58	351	3	Yamashina and Murai [1975]
40	Kawazu	Aug. 17, 1976	5.4	34.8	139.0	0	JMA	167	1	26	19	Abe [1978]
41	Izu-Oshima	Jan. 14, 1978	6.8	34.8	139.2	4	Shimazaki and Somerville [1979]	136	7	42	10	Shimazaki and Somerville [1979]

* Earthquake data is from the supplementary volumes (1 to 3) of the Seismological Bulletin of the JMA [1958, 1966 to 1968] for the years 1926-1967 and from JMA monthly bulletins subsequently except where noted.
† Magnitude determined by Kanamori [1973].

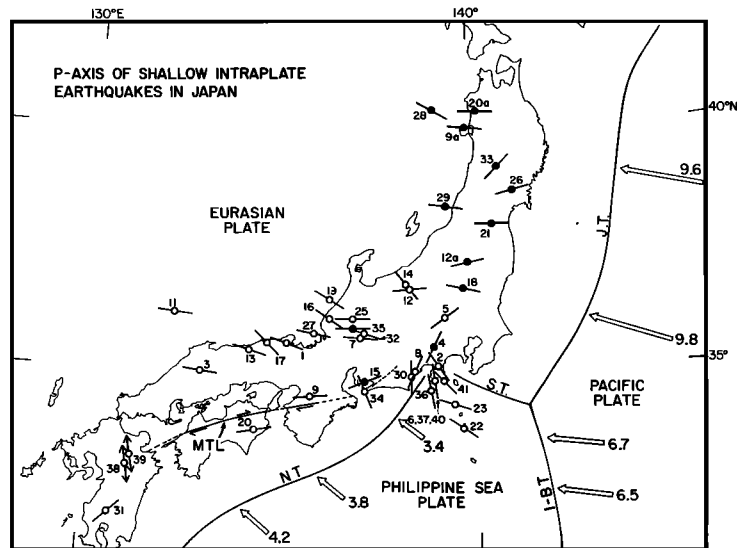


Fig. 3. P axes of intraplate earthquakes with magnitudes of about 6.0 and greater. Epicenters of strike slip and reverse-type faults are denoted by open and solid circles, respectively. The horizontal projection of P axes are shown by lines through epicenter symbols. Numbers adjacent to earthquake symbols correspond to the list of earthquake data for each event presented in Table 1. Events 38 and 39 were normal faults, and the T axes are represented by outward pointing arrows. The Nankai Trough (N.T.), Japan Trench (J.T.), Sagami Trough (S.T.), and Izu-Bonin Trench (I-B.T.) are shown schematically. Relative plate velocities (cm/yr) calculated from Seno [1977] are shown by large hollow arrows. The median tectonic line (MTL) has right-lateral offset (half-sided arrows) and is shown as a solid and dashed line where it has and has not, respectively, been active during the Quaternary.

of three large events there in the last 100 years. The Izu region has been populated for at least the last 400 years. Furthermore, large earthquakes in the Izu region produce shaking of JMA intensity IV as far away as Tokyo, a cultural center for well over 400 years. Hence, the quiescence of the earlier 300-year period appears to be real and not a consequence of an inadequate historical record. The other major contrast is the occurrence of a number of earthquakes adja-

cent to the Bungo Channel area in the earlier 300 years in contrast to none during the more recent period. This was previously noted by Shimazaki [1976]. He concluded, on the basis of the historical development of Japanese civilization, that this must represent true secular variation of seismicity and is probably not a consequence of the population distribution. Aside from these minor differences, this comparison of seismicity patterns suggests that any data missing from the

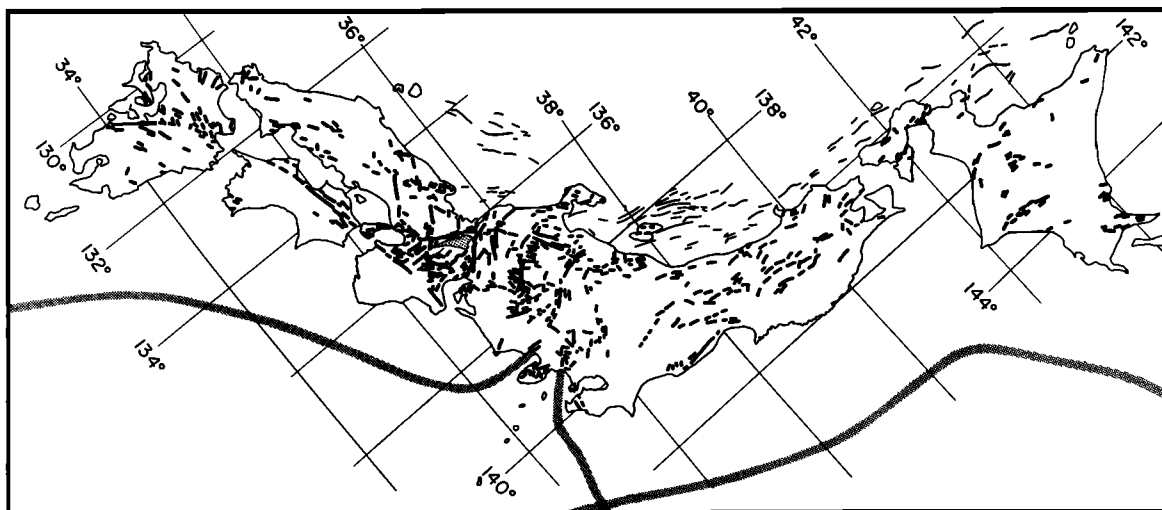


Fig. 4. Distribution of active intraplate faults in Japan. Faults mapped by marine seismic reflection surveys are denoted by thinner lines. Adjacent plate boundaries are represented as thick stippled lines. (Data are adapted directly from Research Group for Active Faults of Japan [1980a, b]).

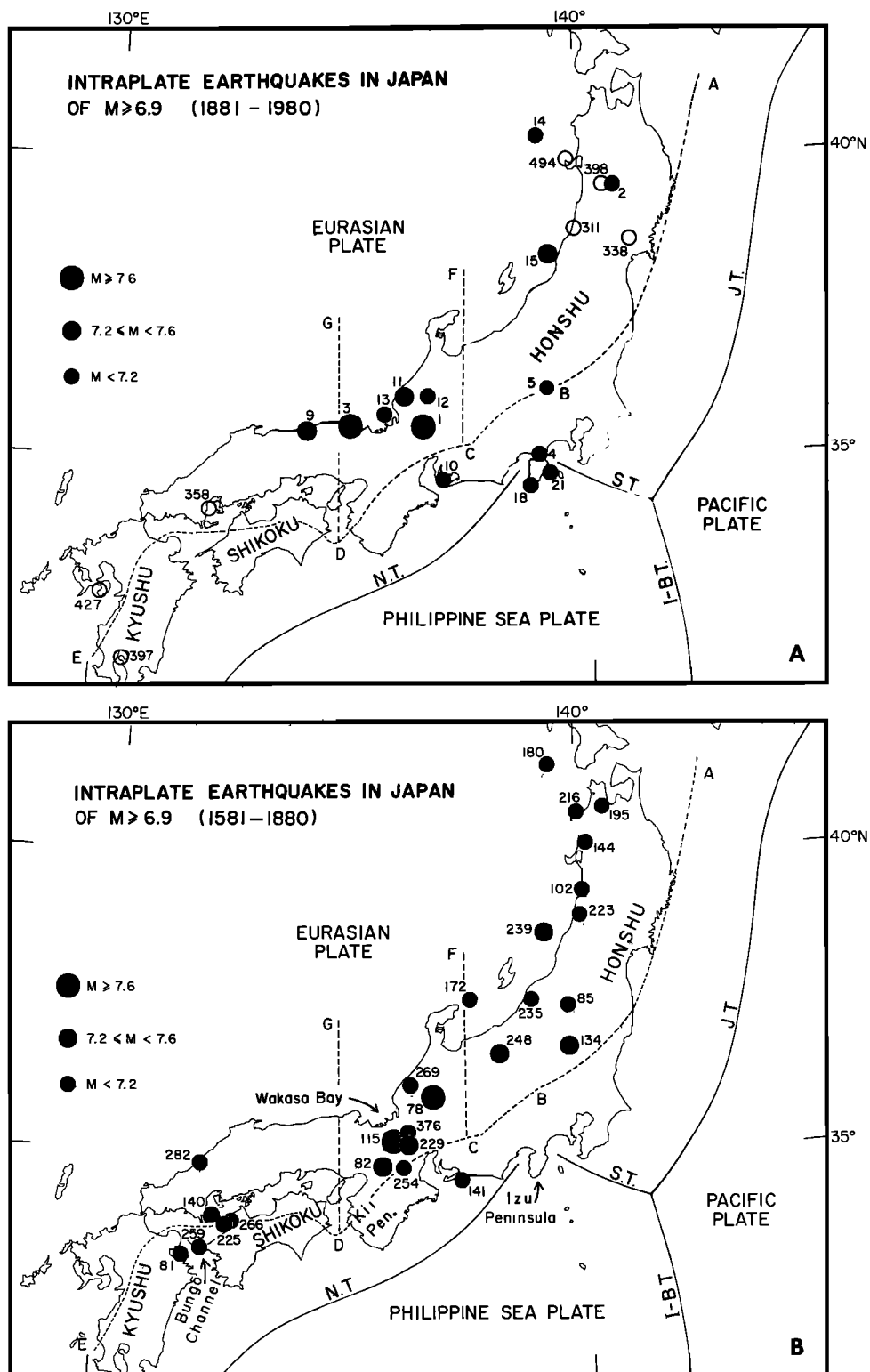


Fig. 5. Intraplate earthquakes in Japan (excluding Hokkaido) of $M > 6.9$ during the period 1881-1980 (Figure 5a) and 1581-1880 (Figure 5b). The radius of the epicenter symbols is proportional to the magnitude of the event. Numbers next to solid symbols in Figures 5a and 5b correspond to Tables 2 and 3, respectively. Numbers adjacent to open symbols in Figure 5a correspond to Table 3. Schematic plate boundaries are given and labeled as in Figure 3. Dashed lines are used to delineate the intraplate regions of Japan. Intraplate Japan is interpreted to be the area northwest of line ABCDE. FC divides northeast Japan from central Honshu. GD divides central Honshu from western Honshu. AB marks the aseismic front which generally parallels the eastern boundary of the aseismic belt [Yoshii, 1975; Yamashina et al., 1978]. The Izu Peninsula region south of BC is characterized by northward compressional tectonics reflecting the recent collision of the Izu Peninsula with Japan in the early Quaternary [Matsuda, 1978; Somerville, 1978]. CDE represents the landward extent of the nascent Wadati-Benioff zone of the Philippine Sea plate [Shiono, 1974]. The region south of ABCDE reflects plate subduction and collisional processes.

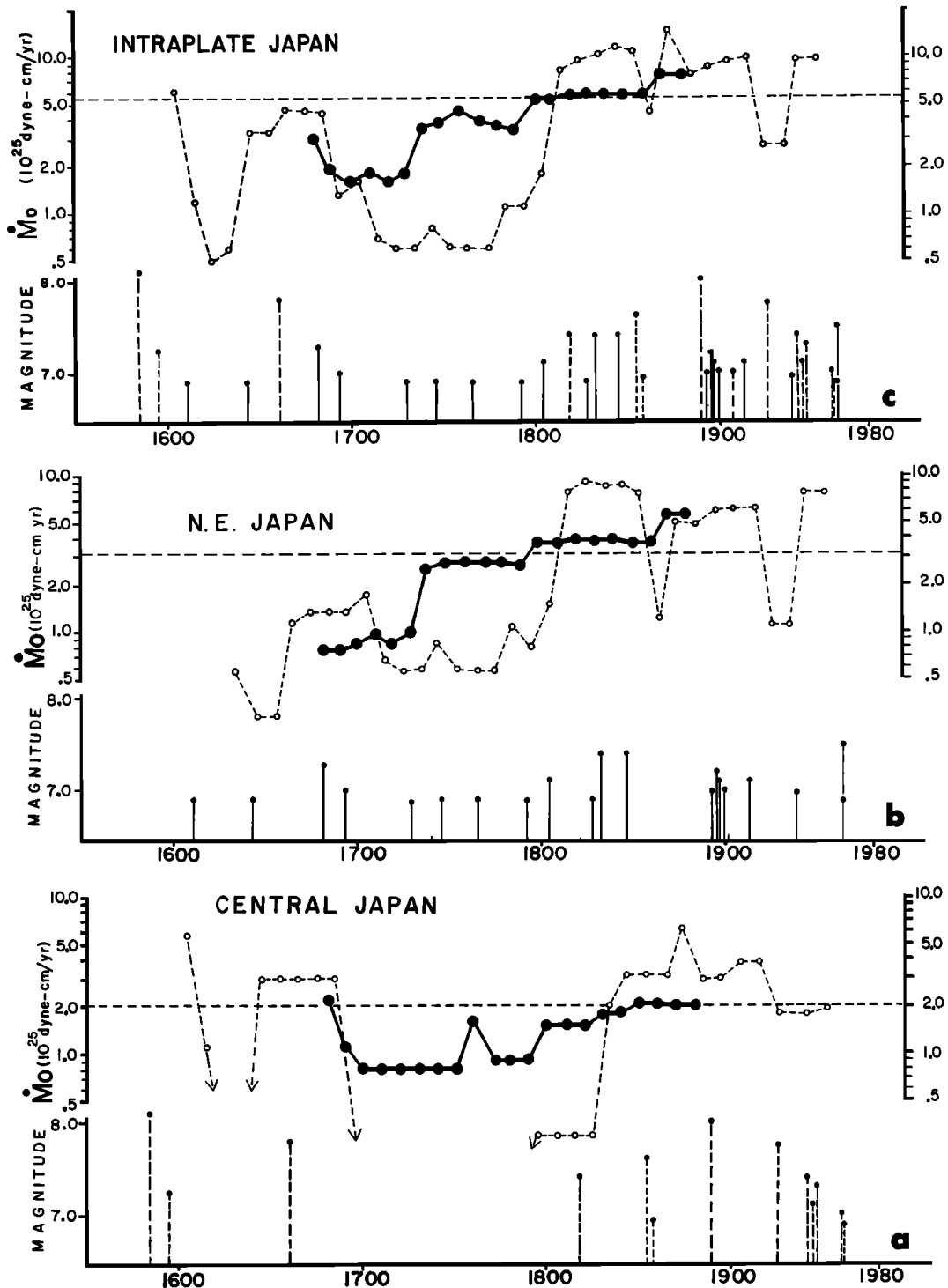


Fig. 6. Earthquakes of $M > 6.9$ as a function of time for intraplate regions of Japan plotted beneath 50-year (small circles) and 200-year (large solid circles) running averages of the seismic moment release rate (10^{25} dyne cm/yr) for each respective region. Data points in the running average curves are placed in the middle of the time period sampled. Moment release rates calculated from the complete 400-year record are shown as horizontal dashed lines. (a) Earthquakes in central Japan (dashed vertical lines). (b) Earthquakes in northeast Japan (solid vertical lines). (c) Earthquakes from both Figures 6a and 6b.

TABLE 2: Intraplate Earthquakes With Known Source Parameters

No.	Name	Date	Latitude 'N	Longitude 'E	M	Ref*	Sec	Fault Type	Fault Length, km	Fault Width, km	Slip, m	Strike#	Dip#	Rake#	M ₀ [‡] , 10 ²⁶ dyne cm	Ref*Region**	
1	Nobi	Oct. 28, 1891	35.6	136.6	8.0	15	'a' 'b' 'c' 'd'	11ds 11ds 11 11ds	80	15	3-9	140 140 140 120	90 90 90 90	45 45 00 53	Total 15 14 4.6 3.7	2,3 CJ	
2	Riku-u	Aug. 31, 1896	39.5	140.7	7.2	15	rds	50	21	4.	4.	0	45	90	14	18	NE
3	Tango	March 27, 1927	35.6	135.1	7.75	4	11	33	13	2.5	2.5	155	90	0	4.6	4	CJ
4	N. Izu	Nov. 25, 1930	35.1	139.0	7.0	1	11	22	12	3.	3.	0	90	0	1.2	5	Izu
							11					27	90	0	1.5		
							11								2.7		
5	Saitama	Sept. 21, 1931	36.15	139.2	7.0	11	11ds	20	10	1.	1.	106	80	355	0.68	11	CJ
6	S. Izu	March 21, 1934	34.8	138.9	5.5	1	r1	7	4	.1	.1	127	90	0	0.01	5	Izu
7	Shizuoka	July 11, 1935	35.0	138.4	6.3		11rds	11	6	1.	20	75	0	20	0.22	16	Izu
8	Shakotan (off)	Aug. 01, 1940	44.4	139.5	7.0	13	rdsr1	170	50	1.1	1.1	0	45	115	20-40	13	HOK
9	Tottori	Sept. 10, 1943	35.5	134.2	7.4	1	r1	33	13	2.5	2.5	80	90	180	3.6	4	WH
10	Mikawa	Jan. 13, 1945	34.7	137.0	7.1	1	rdsr1	12	11	2.5	2.5	180	30	117	.87	6	CJ
11	Fukui	June 28, 1948	36.1	136.2	7.3	1	11	30	13	2-2.5	2.5	350	90	0	3.3	4	CJ
12	Kita-Mino	Aug. 19, 1961	36.1	136.7	7.0	1	11rds	12	10	2.5	2.5	215	60	130	0.9	7	CJ
13	Wakasa-Bay	March 26, 1963	35.8	135.8	6.9	8	11rds	20	8	.6	.6	54	68	158	0.33	8	CJ
14	Oga Pen. (off)	May 7, 1964	40.4	139.1	6.9	12	rds	50	20	1.2	1.2	211	40	90	4.3	13	NE
15	Niigata	June 16, 1964	38.4	139.3	7.5	1	rds	80	30	3.3	3.3	189	56	90	32	9	NE
16	Gifu	Sept. 9, 1969	35.8	137.1	6.6	1	11	18	10	.6	.6	330	90	0	0.35	14	CJ
17	Akita	Oct. 16, 1970	39.2	140.7	6.2	1	11rds	14	8	.65	.65	171	46	119	0.22	17	NE
18	Izu-Hanto-Okii	May 8, 1974	34.6	138.8	6.9	10	rlds	18	8	1.2	1.2	308	80	190	0.59	5	Izu
19	Amagi	July 9, 1974	34.8	138.9	4.9	5	11	18	8	.09	.09	37	90	10	0.003	5	Izu
20	Kawazu	Aug. 17, 1976	34.8	139.0	5.4	1	rlds	3.5	3	.20	.20	304	82	173	0.02	5	Izu
21	Izu-Oshima	Jan. 14, 1978	34.8	139.2	6.8	10	rlds	17	10	1.8	1.8	270	85	188	1.1	10	Izu

*References for data: (1) Usami [1975] and/or Seismology Bulletin of JMA, (2) Mikumo and Ando [1976], (3) Matsuda [1974], (4) Kanamori [1973], (5) Abe [1978], (6) Ando [1974a], (7) Kawasaki [1975], (8) Abe [1974], (9) Abe [1975b], (10) Shimazaki and Somerville [1979], (11) Abe [1975a], (12) International Seismological Centre, (13) Fukao and Furumoto [1975], (14) Mikumo [1973], (15) Utsu [1979], (16) Takeo et al. [1979], (17) Mikumo [1974], (18) Thatcher et al. [1980].

†Fault types: left-lateral strike slip (ll); right-lateral strike slip (rl); reverse dip slip (rds); left-lateral with normal dip slip component (llds); right-lateral strike slip with normal dip slip component (rllds); right-lateral strike slip with reverse dip slip component (rlds), reverse dip slip with right-lateral strike slip component (rdsrl).

‡Fault orientation (strike and dip) and direction of slip (rake) are measured in degrees following conventions used by Aki and Richards [1980].

§The Nobi (1891) and N Izu (1930) earthquakes were associated with multiple faults. The moments of these earthquakes are considered to be the sum of the contributions from each of the fault segments. Sections 'a', 'b', 'c', and 'd' refer to the average divisions of the 1891 Nobi event described by Mikumo and Ando [1976], using Matsuda's [1974] field observations.

**Central Japan (CJ); northeast Japan (NE); Izu Peninsula region (IZU); Hokkaido (HOK); western Honshu (WH). See Figure 10 for division between tectonic regions.

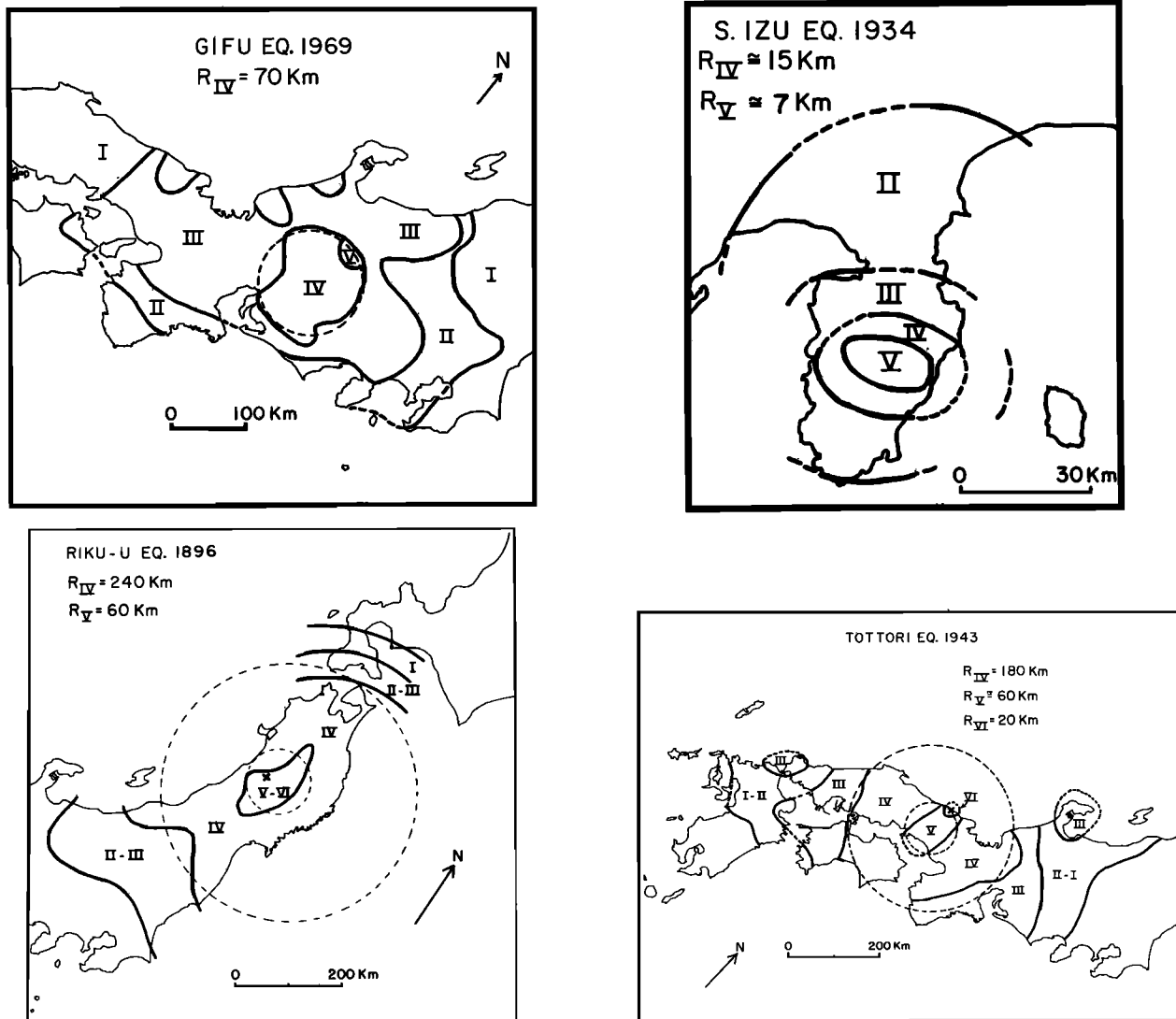


Fig. 7. Maps of JMA intensity from Usami [1975] for four of the earthquakes used in this study. Source parameters of these earthquakes are listed in Table 2. The radius of the circle used to approximate the area of intensity is given. Note that the scale differs for each map.

historical record do not introduce any spatial distortion into the observed pattern of seismicity.

Seismic Moment of Historical Earthquakes

It is necessary to have a quantitative measure of both the moment (M_0) and appropriate focal mechanism for each intraplate earthquake in order to establish the resulting permanent strain deformation. The moment tensors (\bar{M}) of virtually all large earthquakes for the last 100 years have been determined with detailed study of instrumental, geodetic, and geologic data (Table 2). We use information obtained from the areal distribution of seismic intensity, focal mechanisms of recent earthquakes, and observation of Quaternary geologic patterns to estimate the moment tensor of the remaining (historical) large earthquakes that occurred during the last 400 years.

Previous investigations have demonstrated a

strong correlation between the areal distribution of modified Mercalli (MM) intensity VI and seismic moment (M_0) [Hanks et al., 1975; Herrmann et al., 1978]. In Japan, seismic intensity is generally described with the Japan Meteorological Agency's (JMA) intensity scale. The JMA scale consists of only eight grades of intensity [see Usami, 1966] as compared to the 12 of the MM scale [Richter, 1958]. JMA IV is approximately equivalent to MM VI [Trifunac and Brady, 1975]. JMA intensity maps are available for all but one of the earthquakes in Table 2 [Usami, 1975; Kayano and Sato, 1974; Murai, 1977; Murai et al., 1978]. For each of these events, the areal distribution of JMA IV, V, and VI, as approximated by a circle around the epicentral area (Figure 7), is compared to the event's M_0 . Figure 8a shows a linear relationship between $\log(M_0)$ and $\log(\text{Area})$ of intensity IV over 4 orders of magnitude in M_0 . All but two of the points plot within a factor of 3.5 of the value of moment

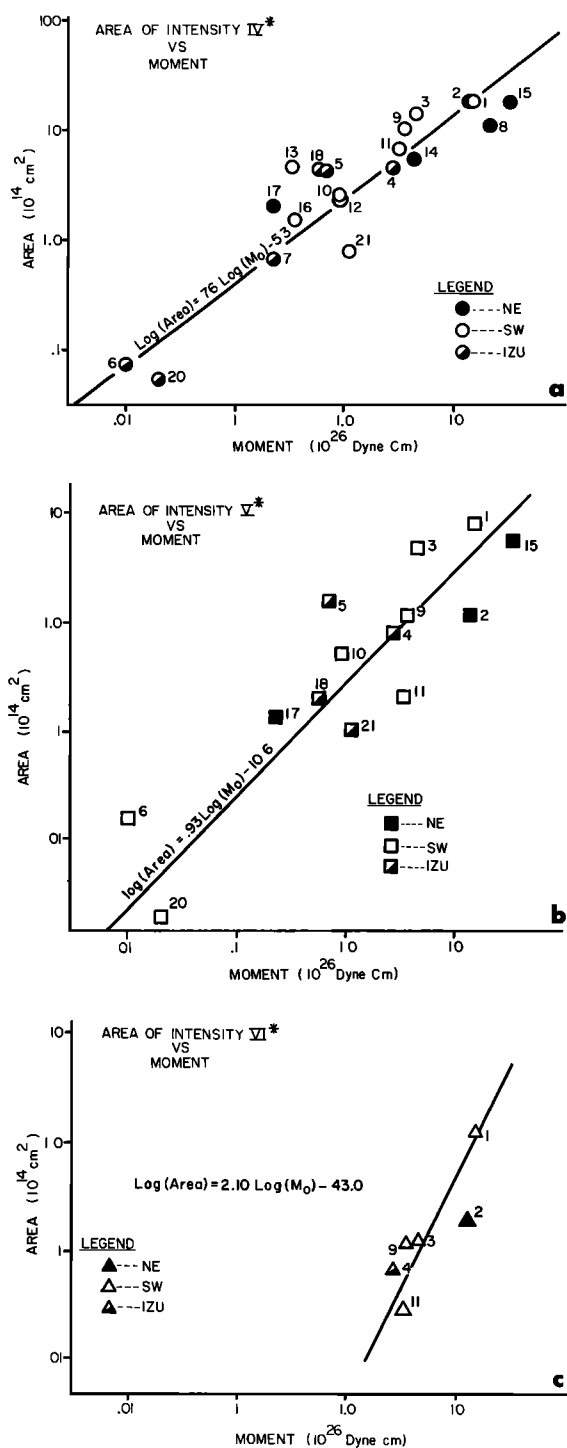


Fig. 8. Plot of seismic moment (10²⁶ dyne cm) versus areal distribution (10¹⁴ cm²) of JMA intensity IV (Figure 8a), JMA intensity V (Figure 8b), and JMA intensity VI (Figure 8c) for intraplate earthquakes in Japan. Open, solid, and half-filled symbols represent earthquakes located in the central, northeast, and Izu regions of intraplate Honshu, respectively. Numbers adjacent to data points correspond to Table 2.

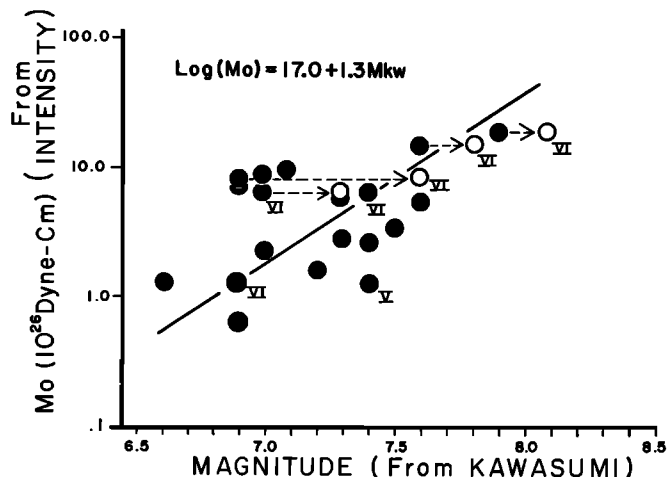


Fig. 9. Magnitudes [from Kawasumi, 1951] versus seismic moment of historical earthquakes in Japan (solid circles). The empirical relations between areal distribution of intensity and moment, established in Figure 8, were used to determine the moments of the historical earthquakes. Values of moment were determined from areal distribution of intensity IV except where noted. The open circles are reestimates of magnitude by Usami [1975], based on intensity data not available to Kawasumi [1951].

predicted by the relation plotted in Figure 8a. A similar relation results for intensities V and VI, although not as many data are available and the scatter is greater (Figures 8b and 8c). The empirical relation in Figure 8a is used to determine the M₀ of historical earthquakes with published isoseismal maps by obtaining the areal distribution of intensity IV. Isoseismals of JMA intensity V and VI (Figures 8b and 8c) are used only when data from JMA IV are not available.

Sufficient data are not available to formulate isoseismal maps for all of the historical earthquakes. Magnitudes of these events, however, have been estimated by Kawasumi [1951] from what seismic intensity data are available. He estimated magnitudes based on his estimate of the seismic intensity at a distance of 100 km from the epicenter. Since the areal distribution of intensity is seen to be a function of seismic moment, it is reasonable to assume that the values of magnitude provided by Kawasumi [1951] should also be proportional to M₀. The magnitudes of large historical earthquakes given by Kawasumi [1951] are compared to their seismic moments in Figure 9, when the latter may be determined with the relations in Figure 8. A simple empirical relation between the two is shown and is used to estimate the moment of large historical earthquakes for which isoseismal maps are not available.

Recent seismicity data and Quaternary geologic data may be used to estimate the focal mechanisms of the historical earthquakes for which no instrumental data are available. The stress system reflected by recent focal mechanisms (Figure 3) and the map of active faults of Japan (Figure 4) has been operative since the beginning of the Quaternary [Research Group for Quaternary Tectonic Map, 1973]. Hence, we assume that

earthquakes during the last 400 years in north-east Japan were of reverse type, similar to the Niigata earthquake of 1964, and those in central and western Japan were of a strike slip nature, similar to the Nobi earthquake of 1891. A general focal mechanism need not be assumed in Shikoku because there is no historical record of large intraplate earthquakes during the last 400 years (see Figure 5). Similarly, the only known large events in the Izu Peninsula occurred recently and their source mechanisms have been studied in detail (Table 2). The moment (M_0), date, and epicentral data of all historical intraplate earthquakes of $M > 6.9$ are presented in Table 3.

Rates of Moment Release and Crustal Shortening From Seismicity Data

We treat the Izu Peninsula, and the northeast, central, and western regions of Honshu separately because of their distinct tectonic styles. The areal dimensions of the deforming volume in each intraplate region (Figure 10a) are chosen as follows: Northeast Honshu: 575 km north-south and 190 km east-west; central Japan: 225 km north-south and 255 km east-west; western Honshu: 125 km north-south and 340 km east-west; Izu Peninsula: 75 km north-south and 35 km east-west. The thickness of the seismogenic volume is placed at 15 km. For each region, the moment tensor (\bar{M}) of all large earthquakes (Tables 2 and 3) are rotated to a north-east-vertical reference frame and summed to obtain $\Sigma\bar{M}$. The strain rate ($\dot{\epsilon}$) of each region is found by substituting $\Sigma\bar{M}$ into equation (3). We consider only strains in the horizontal and vertical directions. An estimate of the rate of permanent crustal shortening (or extension) is also computed by multiplying rates of the maximum horizontal strain times the distance across the deforming area in the respective directions of maximum strain. Computations are performed with both the recent 100-year and complete 400-year records of seismicity. The results are summarized in Table 4 and discussed below. Rates of horizontal deformation obtained from the 400-year history of seismicity are also shown in Figure 11a.

The principal direction of shortening in central Japan is about 95° east of north. \dot{M}_0 computed from the 400-year record of seismicity is 2.1×10^{25} dyne cm/yr. Rates of maximum horizontal compressive strain and crustal shortening, calculated from the 400-year data set are 2.6×10^{-8} /yr and 6.7 mm/yr, respectively. The release of seismic moment occurs as discrete units during earthquakes. If the average values determined above are to be considered representative of secular rates, it is important that the time period sampled be of sufficient length. In Figure 6a the historical record of large earthquakes in central Japan is plotted beneath 50- and 200-year running averages of \dot{M}_0 . The large variation in values of \dot{M}_0 in the 50-year curve clearly shows that a 50-year sample does not provide an accurate estimate of the long-term average of \dot{M}_0 . The 200-year curve, in contrast, is much flatter and values of \dot{M}_0 are generally limited between 1 to 2×10^{25} dyne cm/yr. This suggests that the 400-year record of seismicity provides a sufficient time window for assessment

of secular rates of moment release and crustal shortening.

Crustal shortening in northeast Japan is maximum in a direction about 100° east of north (Figure 11a). \dot{M}_0 averaged over the last 400 years, is 3.2×10^{25} dyne cm/yr (Table 4). The maximum rate of horizontal compressive strain and equivalent crustal shortening computed with the 400-year average of \dot{M}_0 are 2.7×10^{-8} /yr and 5.3 mm/yr, respectively (Figure 11a). Similar to central Japan, the 50-year running average of \dot{M}_0 shows large excursions from the 400-year average of \dot{M}_0 (Figure 6b). In contrast to central Japan, the 200-year running average of \dot{M}_0 is not flat in character but rather shows greater variation, ranging from 0.7 to 5×10^{25} dyne cm/yr as more recent time periods are sampled. Hence, 200 years appears to be too short a time period to estimate accurately secular \dot{M}_0 in northeast Japan. The Niigata earthquake of 1964 ($M_0 = 3.2 \times 10^{27}$ dyne cm) accounts for about 25% of the total moment release in northeast Japan during the last 400 years. Though a 200-year period appears insufficient, hypothetical addition or deletion of a Niigata-type earthquake to the historical record alters the 400-year average of \dot{M}_0 by only 25%. This lends confidence to the hypothesis that the 400-year average of \dot{M}_0 is representative of long-term rates.

Only two intraplate earthquakes are historically recorded in western Honshu (Figure 5). The net moment release of these two earthquakes when averaged over the last 400 years indicates \dot{M}_0 equal to 3.4×10^{24} dyne cm/yr. Rates of horizontal strain and crustal shortening calculated from these data are maximum in an easterly direction and equal 0.6×10^{-8} /yr and 2.0 mm/yr, respectively. Estimates of secular \dot{M}_0 in a region of such low seismic activity are susceptible to large error. Hence, the above rates of strain and strain shortening cannot with any confidence be considered representative of secular deformation rates.

Shikoku has been aseismic during historic time except for a group of earthquakes located in the vicinity of the Bungo Channel (Figure 5). Recent smaller earthquakes in this region are commonly located relatively deep (40-60 km), show normal faulting, and have been interpreted to reflect complex interplate processes associated with the leading edge of the subducting Philippine Sea plate [Shiono and Mikumo, 1975]. The large historical earthquakes located in the Bungo Channel region are not associated with any evidence of surface faulting and very likely were situated at depth. Hence, there is no evidence of intraplate type seismicity in Shikoku during the last 400 years.

Three large earthquakes have occurred in the Izu Peninsula this century: The North Izu event ($M = 7.0$) of 1930, the Izu-Hanto-Oki shock ($M = 6.9$) of 1974, and the Izu-Oshima ($M = 6.8$) earthquake of 1978. The only large historical earthquake to be confidently located on the Izu Peninsula is believed to have occurred on the Tanna fault in 841 A.D. [Usami, 1966; Somerville, 1978]. The Tanna fault exhibited surface breakage during the 1930 North Izu earthquake. This suggests a 1000-year recurrence time for earthquakes of about $M \approx 7$ on the Tanna fault [Somerville, 1978]. Data from recent excavations

TABLE 3. Intraplate Earthquakes, 1580 to Present, of Magnitude Greater Than or Equal to 6.9 for Which Instrumentally Determined Source Parameters are Not Available.

Epicentral Data					
No. †	Date	Latitude °N	Longitude °E	Magnitude	Moment‡, 10 ²⁶ dyne cm
<u>Northeast Japan: 1581-1880</u>					
85	Sept. 27, 1611	37.5	139.7	6.9	1.4*
102	Oct. 18, 1644	39.4	140.1	6.9	1.4*
134	Jan. 18, 1683	36.75	139.65	7.3	4.8*
144	June 19, 1694	40.2	140.2	7.0	1.9*
172	Aug. 1, 1729	37.6	137.6	6.9	1.4*
182	May 14, 1746	(37)	(140)	6.9	1.4*
195	March 8, 1766	49.3	140.6	6.9	1.4*
216	Feb. 8, 1793	40.85	139.95	6.9	1.4*
223	July 10, 1804	39.05	139.95	7.1	2.6*
235	Dec. 18, 1828	37.6	138.9	6.9	3.6 (VI)
239	Dec. 7, 1833	38.9	139.15	7.4	32.0
248	May 8, 1847	36.7	138.2	7.4	6.5 (VI)
					sum = 59.8
<u>Northeast Japan: 1881-1980</u>					
311	Oct. 22, 1894	38.9	139.9	7.0	3.3 (IV)
338	May 12, 1900	38.7	141.1	7.0	6.9 (IV)
398	March 15, 1914	39.5	140.4	7.1	4.1 (IV)
494	May 1, 1939	40.0	139.8	7.0	1.3 (IV)
					sum = 15.6
<u>Central Japan: 1581-1880</u>					
78	Jan. 18, 1586	36.0	136.8	8.1	19.0 (VI)
82	Sept. 5, 1596	34.85	135.75	7.25	6.3 (VI)
115	June 16, 1662	35.25	136.0	7.8	15.0 (VI)
229	Aug. 2, 1819	36.2	136.3	7.4	1.3 (V)
254	July 9, 1854	34.75	136.0	7.6	8.5 (VI)
269	April 9, 1858	36.2	136.3	6.9	7.6 (VI)
					sum = 57.7
<u>West Honshu: 1581-1880</u>					
81	** Sept. 4, 1596	33.3	131.7	6.9	1.4*
140	** Jan. 4, 1686	34.1	132.3	7.0	8.7 (V)
225	** Apr 21, 1812	33.3	132.5	6.9	1.4*
259	** Dec. 26, 1854	33.4	132.1	7.0	1.9*
266	** Oct. 12, 1857	33.9	132.7	6.9	1.4*
282	March 14, 1872	34.9	132.0	7.4	10.0 (VI)
					sum = 24.8
sum (minus Bungo Channel events) = 10.0					
<u>West Honshu: 1881-1980</u>					
358	** June 2, 1905	34.2	132.3	6.9	5.3 (IV)
					sum = 5.3
sum (minus Bungo Channel events) = 0.0					

*The relation between magnitude (M_{kw}) and moment (M_o) in Figure 9 was used to determine the seismic moment.

†Number of each event corresponds to that listed in Usami's [1975] catalogue. The November 25, 1614 earthquake (M=7.7, lat=37.5N, long=138.1E) listed in Usami [1975] is not included because Hagiwara et al. [1980] re-examined the historical data and found that the event is probably much smaller with M=6.3.

‡Seismic moment is determined from the areal distribution of JMA Intensity with the relations shown in Figure 8 except for those values denoted by a single asterisk. The scale of intensity used is given in parentheses. We assume on the basis of similar intensity patterns that Event No. 239 produced the same seismic moment as the June 16, 1964 Niigata earthquake [see Hatori and Katayama, 1977].

**Events located in or near the Bungo Channel.

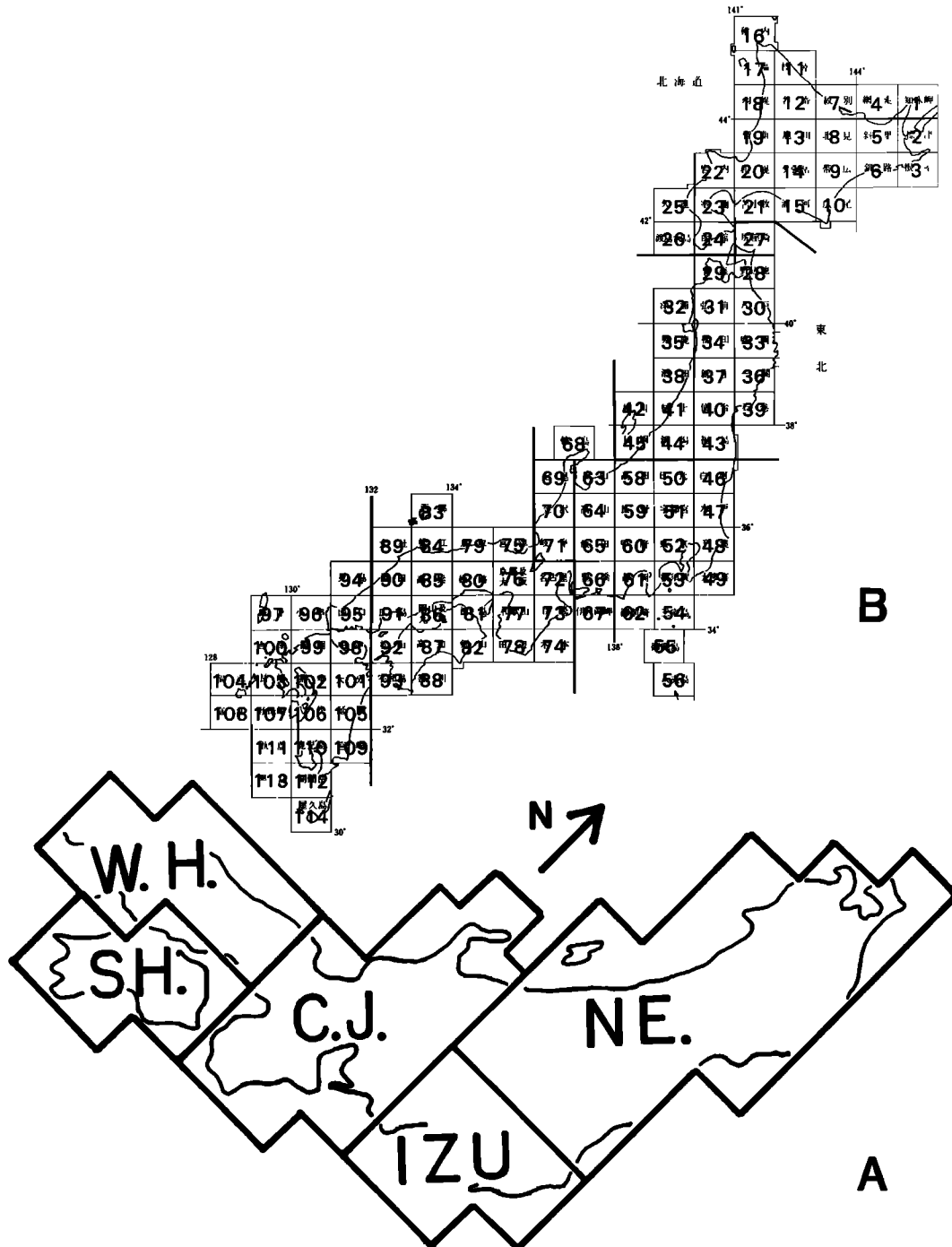


Fig. 10. (a) Index map of regions discussed in this study: northeast Japan (NE), central Japan (CJ), western Honshu (WH), Shikoku (SH), Izu Peninsula and adjacent environs (IZU). (b) Number is index location of maps referred to in Table 5 and the active faults book [Research Group for Active Faults of Japan, 1980a, b].

across the Tanna fault are in accord with this estimate [Matsuda et al., 1981]. If we assume a 1000-year recurrence time for each of the three earthquakes that occurred on the peninsula during this century, calculations produce an average moment release rate of 4.4×10^{23} dyne cm/yr. Converting \dot{M} to rates of strain indicates that the Izu Peninsula is shortening in a northwesterly direction at rates of 1.3 mm/yr, equivalent

to a horizontal compressive strain rate of 1.4×10^{-8} /yr.

Deformation Rates From Quaternary Fault Data

Data and Assumptions

The recent publication of 'Active Faults in Japan: Sheet Maps and Inventories' [Research

TABLE 4. Summary of Intraplate Deformation Rates Determined With Seismologic Data

Time Period	Mechanism *	Moment, 10 ²⁵ /yr dyne cm	Shortening			Extension		
			Strain Rate, 10 ⁻⁸ /yr	Rate, mm/yr	Azimuth, deg	Strain Rate, 10 ⁻⁸ /yr	Rate, mm/yr	Azimuth, deg
<u>Northeast Japan</u>								
1881-1980	Niigata (1964)	6.6	5.7	11.1	100	6.0	0.1	vertical
1581-1980	Niigata (1964)	3.2	2.7	5.3	100	2.9	0.4	vertical
<u>Central Japan</u>								
1881-1980	Nobi 'a' (1891)	2.5	3.4	8.7	100	3.1	7.1	10
1581-1880	Nobi 'a' (1891)	2.1	2.6	6.7	95	2.6	5.8	5
<u>West Honshu</u>								
1881-1980	Nobi 'a' (1891)	1.0	0.9	3.5	125	0.9	1.3	35
1581-1880	Nobi 'a' (1891)	0.34	0.6	2.0	105	0.6	0.1	15
<u>Izu Peninsula</u>								
981-1980	none	0.044	1.4	1.3	150	1.4	0.6	60

*The focal mechanism assumed for historical earthquakes. See Table 2.

Group for Active Faults of Japan, 1980a, b] (hereinafter referred to as the 'active faults book') provides for the first time detailed data of uniform quality describing all active Quaternary faults in Japan. Faults listed and mapped at 1:200,000 (Figure 10b) in the active faults book were recognized primarily by interpretation of aerial photographs supplemented by geological maps. Major faults were checked in the field. Each map is supplemented by a table detailing, as available, the strike, dip, length, total displacement, and average rate of slip of each fault in that area. Each fault is also classified in terms of its 'certainty': (I) Certain beyond doubt that the fault was active during the Quaternary, (II) though not definitely certain of the age of the offset features, it is possible to infer the sense of displacement and the fault is generally considered to have been active during the Quaternary (T. Matsuda, personal communication, 1981), (III) the fault is a mere lineament only suspected to be active during the Quaternary.

The data in the active faults book provides most of the information necessary to describe the average rate of seismic moment release (\dot{M}) of each Quaternary fault. Assumptions need only be made when assigning a value for the shear modulus ($\mu = 3 \times 10^{11}$ dyne/cm²), the dimension of fault width (W) and in those cases where information on fault dip (θ) is not available. Those faults listed without information of the dip, but identified as dip slip faults, are assumed to be reverse type (rake = 90°) and to dip at 45°. Similarly, strike slip faults without dips specified are assumed to dip at 90° and have a rake of

0° (left lateral) or 180° (right lateral). The parameter of fault width is assigned as follows: (1) faults of length >15 km are given a fault width of 15 km/sin(θ) (they break through the entire seismogenic thickness), (2) faults of length <15 km with total displacements <5 m are assumed to have equidimensional fault areas, (3) faults of length <15 km with displacements of >5 m are assigned a fault width of 15 km/sin(θ) (they break through the entire seismogenic thickness). Earthquakes of length greater than 15 km, particularly those with slip greater than 2-2.5 m, generally have a fault width approaching 15 km (the seismogenic thickness) or greater (Table 2). Since all faults of length >15 km in the active faults book have displacements >5 m, assumption 1 is reasonable. Assumption 2 is justified by looking at the source dimensions of smaller earthquakes (length <15 km) (Table 2). The width of these smaller earthquake ruptures is usually about the same as the length. Hence, a conservative manner in which to estimate the source dimensions of those geologic faults, with length <15 km and $u < 5$ m, is to assume (assumption 2) that they are equidimensional (width = length). Many geologic faults of 1- to 15-km length are listed in the active faults book with displacements of the order of tens of meters. Average displacements associated with even the largest earthquakes in Table 2 reach to only a few meters, and furthermore, these large earthquakes generally have fault lengths >20 km. Hence, it is not common for earthquakes with a fault length of <15 km to have displacements >5 m. Instead it is more reasonable to assume that the short fault segments with the larger

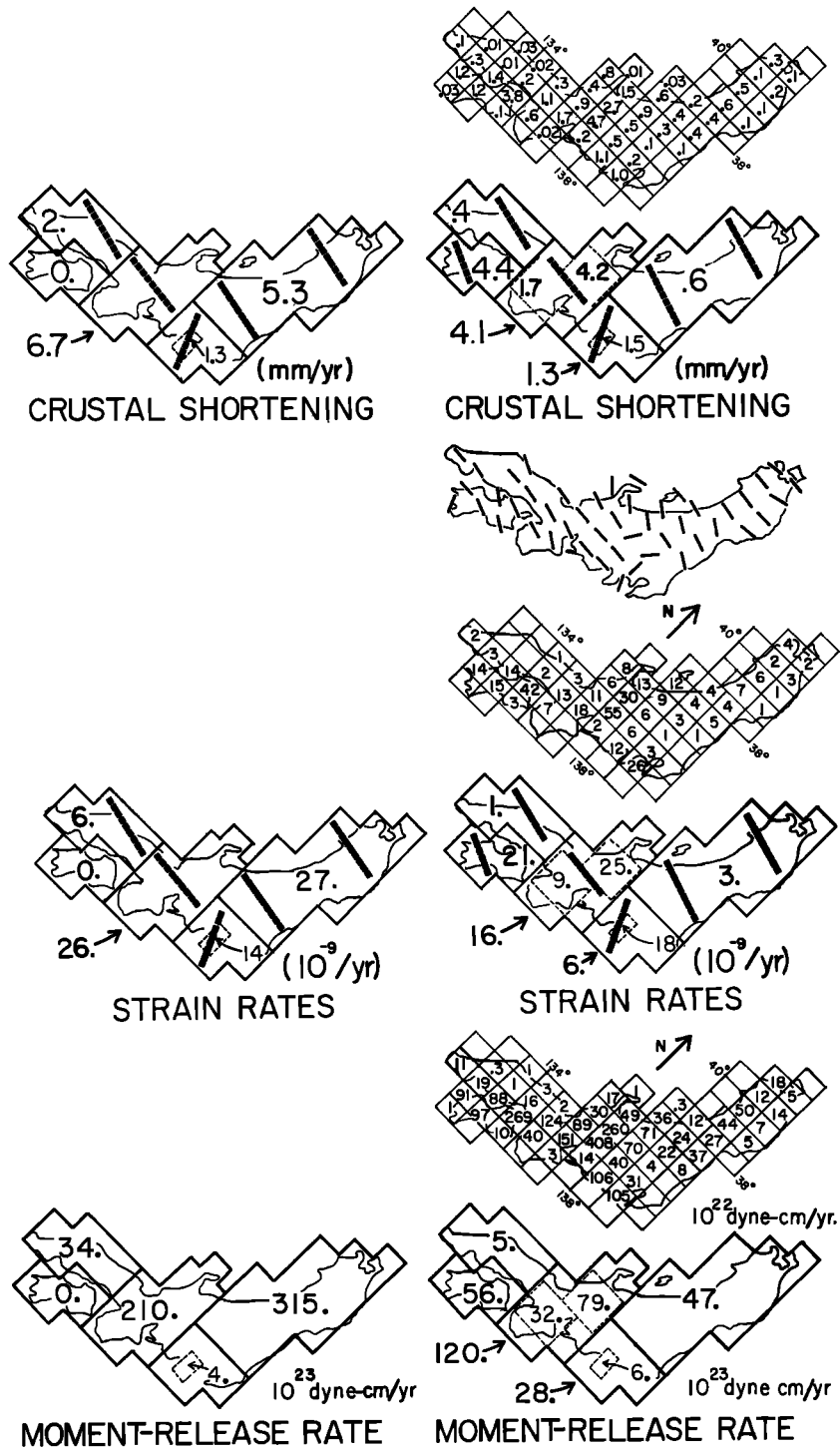


Fig. 11a

Fig. 11b

Fig. 11. (a) Regional (see Figure 10a) averages of the rates of moment release, horizontal compressive strain, and crustal shortening calculated from the 400-year record of seismicity. Supposition that these values are representative of secular rates is dependent on the rate of seismicity as well as the quality of the historic record of earthquakes in each respective region. Each area is discussed separately in the text. Principal directions of horizontal compressive strain and shortening are denoted by dashed bars. Note that the values in the Izu region are computed only from seismicity within the small dashed box that encloses the Izu Peninsula. No estimate is given for the Izu region as a whole because proximity to plate boundaries negated confident identification of historical intraplate earthquakes. (b) Case 2 regional (see Figure 10a) and grid-by-grid (see Figure 10b) averages of the rates of moment release, horizontal compressive strain, and crustal shortening calculated from slip rates of active faults on land. Valid comparison of these values with rates obtained from the 400-year record of seismicity presented in Figure 11a is conditional to the distribution of seismicity, the regional geology, and the style and rate of faulting in each respective region. See text for further discussion. Principal directions of horizontal compressive strain for the larger intraplate regions and smaller grids are shown by dashed bars and thin solid lines, respectively. Smaller numerals within the region of central Japan give average rates for the local areas enclosed by the dashed boxes.

(>5 m) displacements listed in the active faults book are the result of many earthquakes occurring along a major fault of which only a small portion is presently visible at the surface. Faults with such large displacements probably cut through the entire seismogenic thickness of the crust (assumption 3). We use these assumptions and the data provided in the active faults book to calculate the average rate of moment release (\dot{M}) for each active Quaternary fault.

Rates of Moment Release and Crustal Shortening Estimated from Slip Rates on Quaternary Faults

Average rates of slip on a geologic fault may be estimated only when the age of geologic and geomorphologic features offset by the fault are known. Slip on active faults in Japan is generally evidenced by the displacement of low-relief surfaces that formed by either fluvial or marine deposition and erosion during the Quaternary. Tephra and organic matter in these terraces may be dated with radiometric techniques, and hence the age of the displaced surfaces determined. The dates of fault offsets listed in the active faults book are prevalently less than about 200,000 years of age. Hence, values of slip rate in the active faults book provide us directly with information of the average rate of deformation in Japan during the late Quaternary.

Specific values of slip rates are given in the active faults book only when the ages of displaced features have been quantitatively determined. In many cases the precise age of displaced geologic markers is not known but can be constrained within certain limits. In such cases, the active faults book provides estimates of the 'degree' of slip rate: degree 'A,' 1-10 mm/yr; degree 'B,' 0.1-1 mm/yr; degree 'C,' 0.01-0.1 mm/yr. The moment release rate (\dot{M}) may thus be defined for all faults listed in the active faults book once a specific numerical value of slip rate is assigned to those faults with slip rates categorized only as degree 'A,' 'B,' or 'C.' Three cases are considered here: Case 1, faults of degree 'A,' 'B,' and 'C' slip at 1 mm/yr, 0.1 mm/yr, and 0.01 mm/yr, respectively; case 2, faults of degree 'A,' 'B,' and 'C' slip at 5 mm/yr, 0.5 mm/yr, and 0.05 mm/yr, respectively; case 3, faults of degree 'A,' 'B,' and 'C' slip at 10 mm/yr, 1 mm/yr, and 0.1 mm/yr, respectively. For each case, the moment release rate (\dot{M}) of faults of certainty I and II are summed, and formula (3) is used to calculate the principal directions and rates of horizontal strain of each intraplate region.

The longer time base of the Quaternary fault data allows us to view the deformation process with greater detail than with historic seismicity data. The results of the deformation analysis for faults of certainty I and II, for each individual map (Figure 10b) and larger intraplate regions (Figure 10a), are summarized in Table 5. \dot{M}_0 for each intraplate region, when only faults of certainty I are considered, is also for the sake of comparison listed in Table 5. Confidence limits on rate estimates for each region may be obtained by comparing case 2 results to the range of values defined by cases 1 and 3 in Table 5. Results for case 2 are pictorially presented in Figure 11b. In general, the average rates of

moment release, when cases 1 and 3 are assumed, do not vary by more than a factor of 2 from rates calculated assuming case 2 (Table 5). The results thus appear quite stable and are not greatly dependent on the estimates of slip rate assumed for those faults without specified slip rates but categorized only as degree 'A,' 'B,' or 'C.'

Comparison of the Average Rates of Deformation Determined From Seismicity and Quaternary Fault Data

A valid comparison of values of \dot{M} estimated from the seismicity and geologic data sets is strongly dependent on the quality of the geologic record of offsets. In this section, values of \dot{M} calculated from the two data sets are compared and discussed with regard to the distribution of seismicity, the style and rate of faulting, and the regional geology. The best estimates of secular \dot{M}_0 , and the horizontal rates of strain and crustal shortening are then provided for each region in Figure 12.

In central Japan, the seismicity is concentrated on land (Figure 5), faulting is generally strike slip (Figure 4), there is very little sedimentary cover [Research Group for Quaternary Tectonic Map, 1973], and large earthquakes generally produce observable surface ruptures along mappable geologic faults [e.g., Matsuda, 1977]. Both the seismicity and fault data indicate that central Japan (grids 63-78) is being compressed in an easterly azimuth. \dot{M}_0 estimated from Quaternary fault data ranges from 0.6 to 1.9×10^{25} dyne cm/yr (Table 5). \dot{M}_0 (2.1×10^{25} dyne cm/yr) computed from the 400-year record of seismicity lies just at the upper bound of the range of values constrained by the geologic data. Similarly, seismologically determined rates of horizontal compressive strain and crustal shortening (2.6×10^{-8} /yr and 6.7 mm/yr, respectively) are at the high end of the range of rates determined geologically (0.9 to 2.6×10^{-8} /yr and 2.2 to 6.6 mm/yr). Qualitative examination of data in Figure 8 indicates that estimates of \dot{M}_0 for historical earthquakes are on average limited to a factor of 2 to 3. When such errors in the computation of \dot{M}_0 from the 400-year record of seismicity are considered, the slightly larger rates determined seismologically should not be considered significant. We may arrive at a similar conclusion from geologic considerations. Aseismic creep has not been observed on any active faults in Japan except for relatively minor amounts of fault slip immediately after great earthquakes [Matsuda, 1977]. The geologic record of fault offsets should then at best, if perfectly preserved and recognized, yield estimates of deformation rates equal to those obtained from seismicity data. More likely is that fault offsets are not perfectly preserved and, hence, not always recognized. The geologic data will thus probably yield a minimum estimate of \dot{M}_0 . Noting that slip rates on Quaternary faults are generally estimated from displacement of features between 10,000 and 200,000 years old, the similarity of the values obtained from the two data sets strongly suggests that the mode and rate of deformation in central Japan has been steady through the late Quaternary.

TABLE 5. Rates of Crustal Shortening Estimated From Slip Rates on Faults of Certainty I and II.

Grid*	Areal Dimension†, km		Case 1§			Case 2**			Case 3††			
	NS	EW	Moment‡, 10 ²³ /yr dyne cm/yr	Strain, 10 ⁻⁹ /yr	Rate, mm/yr	Moment‡, 10 ²³ /yr dyne cm/yr	Strain, 10 ⁻⁹ /yr	Rate, mm/yr	Moment‡, 10 ²³ /yr dyne cm/yr	Strain, 10 ⁻⁹ /yr	Rate, mm/yr	Azimuth, deg
28	75	40	1.1	0.4	0.01	0.5	1.7	0.1	1.1	3.5	0.1	95
29	60	85	0.5	0.9	0.07	1.8	3.5	0.3	3.5	6.6	0.6	80
30	75	60	0.3	0.6	0.03	1.4	3.1	0.2	2.8	6.3	0.4	80
31-32	75	85	0.3	0.4	0.04	1.2	1.7	0.1	2.2	3.2	0.3	100
33	75	85	0.2	0.3	0.02	0.7	1.0	0.1	1.3	1.9	0.2	90
34-35	75	85	1.9	2.3	0.2	5.0	5.5	0.5	8.8	9.7	0.8	100
36	75	60	0.2	0.4	0.03	0.5	1.0	0.1	0.9	1.8	0.1	85
37-38	75	90	1.2	1.5	0.1	4.4	6.1	0.6	8.5	11.8	1.1	100
39	-	-	-	-	-	-	-	-	-	-	-	-
40	75	85	1.1	1.6	0.1	2.7	3.9	0.4	4.7	6.8	0.7	120
41	75	45	0.6	1.7	0.1	1.2	3.9	0.2	2.0	6.7	0.3	115
42	35	25	0.02	0.1	0.003	0.03	0.2	0.01	0.03	0.3	0.01	90
43	75	85	2.5	3.4	0.3	3.7	5.1	0.4	5.3	7.3	0.6	105
44	75	85	1.1	1.6	0.1	2.4	3.7	0.4	4.0	6.4	0.7	120
45	75	40	1.5	4.5	0.2	3.6	11.5	0.6	6.2	20.3	1.0	125
46	75	85	0.2	0.1	0.01	0.8	0.5	0.1	1.6	1.0	0.1	120
50	75	85	2.1	3.3	0.3	2.2	3.4	0.3	2.4	3.6	0.3	100
51	75	85	0.4	0.6	0.06	0.4	0.6	0.1	0.4	0.6	0.06	40
58	75	85	2.4	3.3	0.3	7.1	9.3	0.9	13.0	16.9	1.7	125
59	75	85	1.6	1.3	0.1	7.0	5.8	0.5	13.8	11.3	1.0	32
Average	575	190	18.9 (14)	1.3	0.3	46.6 (28)	3.1	0.6	82.5 (45)	5.4	1.1	105
48	-	-	-	-	-	-	-	-	-	-	-	-
52	75	85	2.4	2.4	0.2	3.1	3.0	0.2	4.1	3.8	0.3	180
53-49	35	95	6.4	13.7	0.5	10.5	26.3	1.0	15.6	38.7	1.5	155
60	75	85	1.7	2.2	0.2	4.0	5.9	0.5	7.0	10.6	0.9	95
61-62	75	85	9.4	12.3	1.1	10.6	12.4	1.1	12.1	12.5	1.1	90
Average	150	170	19.9 (19)	4.2	0.9	28.2 (26)	6.1	1.3	38.8 (36)	8.8	1.7	135
63	75	35	2.1 (2)	4.2	0.3	6.4 (6)	18.4	1.5	11.8 (11)	36.4	2.6	155
64	40	85	1.8	5.0	0.5	4.9	13.4	1.5	8.8	23.9	2.7	130
65	75	85	9.5	12.0	1.0	26.0	30.1	2.7	46.6	55.3	4.8	100
	75	85	30.6	45.3	4.1	40.8	55.0	4.7	53.5	67.2	5.7	90

Northern Japan

Izu Area

Izu Peninsula

Central Japan

66	75	85	0.3	0.4	0.04	1.4	2.1	0.2	2.8	4.2	0.4	95
67	-	-	-	-	-	-	-	-	-	-	-	-
68	20	40	0.04	0.1	0.005	0.1	0.4	0.01	0.1	0.6	0.03	80
69	75	25	0.9	4.2	0.4	1.7	7.9	0.8	2.7	12.6	1.3	135
70	75	65	1.6	3.0	0.2	3.0	6.2	0.4	4.7	10.1	0.7	110
71	75	85	1.9	2.3	0.2	8.9	10.8	0.9	17.6	21.4	1.8	90
72	75	85	4.5	4.9	0.4	15.1	18.3	1.7	28.3	35.5	3.3	110
73	75	65	0.08	0.1	0.01	0.3	0.3	0.02	0.5	0.05	0.6	120
74	-	-	-	-	-	-	-	-	-	-	-	-
75	35	85	0.1	0.9	0.07	0.2	3.0	0.3	0.2	5.7	0.5	100
76	75	85	5.0	6.0	0.6	12.4	12.6	1.1	21.7	21.1	1.8	105
77	75	85	2.8	4.3	0.4	4.0	6.5	0.6	5.4	9.3	0.9	115
78	-	-	-	-	-	-	-	-	-	-	-	-
Average	225	255	59.1 (50)	8.6	2.2	118.8 (95)	16.1	4.1	192.9 (152)	25.5	6.6	95
64-65,70-71	150	170	43.6 (38)	15.3	2.6	78.7 (62)	25.0	4.2	122.0 (106)	37.2	6.4	95
72-73,76-77	150	170	12.4 (9)	3.7	0.7	31.8 (20)	9.4	1.7	55.9 (32)	16.5	3.0	110
<u>West Honshu</u>												
79	35	85	0.04	0.02	0.02	0.3	0.6	0.02	0.4	1.2	0.1	30
80	75	85	1.2	1.8	0.2	1.6	2.1	0.2	2.2	2.7	0.2	100
83	-	-	-	-	-	-	-	-	-	-	-	-
84	20	85	0.004	0.05	0.01	0.1	0.3	0.03	0.1	0.5	0.1	130
85	75	85	0.03	0.03	0.002	0.1	0.1	0.01	0.1	0.3	0.02	95
89-90	75	85	0.01	0.02	0.001	0.03	0.1	0.01	0.1	0.3	0.01	155
91	75	85	0.4	0.7	0.06	1.9	3.3	0.3	3.9	6.6	0.6	100
94	-	-	-	-	-	-	-	-	-	-	-	-
95-96	75	85	0.2	0.4	0.03	1.1	1.7	0.1	2.2	3.4	0.3	90
Average	125	340	1.9 (1.5)	0.4	0.10	5.0 (3)	1.1	0.4	8.9 (5)	1.9	0.7	100
<u>Shikoku</u>												
81	75	85	26.1	40.9	3.7	26.9	42.0	3.8	28.0	43.3	3.9	110
82	75	40	0.9	3.0	0.1	1.0	3.2	0.1	1.1	3.5	0.2	115
86	75	85	8.6	13.5	1.4	8.8	13.8	1.4	9.1	14.1	1.4	125
87	75	85	9.5	15.0	1.3	9.7	15.3	1.2	9.9	15.7	1.2	110
88	-	-	-	-	-	-	-	-	-	-	-	-
92	75	85	1.8	2.9	0.2	9.1	14.4	1.2	18.2	28.8	2.5	90
93	70	45	0.02	0.3	0.03	0.1	0.3	0.02	0.2	0.6	0.1	155
Average	125	200	46.9 (46)	18.2	4.0	55.6 (54)	20.8	4.4	66.5 (64)	24.3	5.1	110

*See Figures 10 for location of each grid and region.
 †Areal dimensions of volume used to calculate strain. Depth of volume is assumed to be 15 km.
 ‡The moment release rate for each grid is the sum of contributions from each fault in that grid. Moment release rates, when only faults of certainty I are considered, are given in parentheses.
 §Faults categorized as only degree 'a', 'b', and 'c' are assumed to slip at 1 mm/yr, .1 mm/yr, and .01 mm/yr, respectively.
 ¶Faults categorized as only degree 'a', 'b', and 'c' are assumed to slip at 5 mm/yr, .5 mm/yr, and .05 mm/yr, respectively.
 ††Faults categorized as only degree 'a', 'b', and 'c' are assumed to slip at 10 mm/yr, 1.0 mm/yr, and .1 mm/yr, respectively.

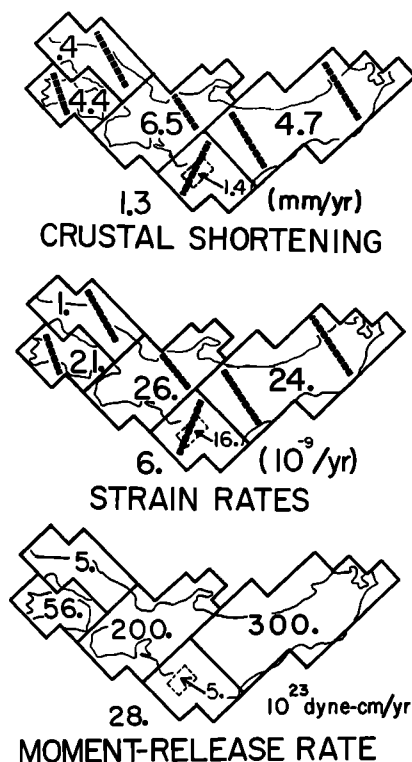


Fig. 12. An integration of data in Figures 11a and 11b showing the best estimates of the long-term averages of the rates of seismic moment release, horizontal compressive strain, and crustal shortening of intraplate regions of Japan.

In northeast Japan, both the geologic and seismicity data indicate that the average trend of maximum horizontal shortening is about due east. The rate of moment release, and hence deformation, estimated from the fault record is, however, 4 to 16 times less than estimates obtained with the seismicity data. The average rate of moment release calculated from the geologic record of fault displacements is 0.2 to 0.8×10^{25} dyne cm/yr in contrast to 3.2×10^{25} dyne cm/yr estimated from the 400-year historical record of seismicity. The large difference in \dot{M}_0 estimated from seismicity and the longer geologic fault record at first sight implies that the rate of faulting in northeast Japan has recently increased dramatically, but closer examination of the geologic data and distribution of seismicity indicates that this is probably not the case.

Northeast Japan, in contrast to central Japan, is largely overlain by Neogene and Pleistocene sediments [Research Group for Quaternary Tectonic Map, 1973] and is characterized by reverse-type faulting. Many faults in northeast Japan may possibly remain unrecognized because they do not completely break through the sedimentary cover. Furthermore, less than 50% of the moment release in northeast Japan during the last 400 years occurred onshore. Thus, a major amount of moment release and crustal shortening in northeast Japan takes place offshore along the Japan Sea coast. This is similarly reflected in the distribution of active faults (Figure 4) and folds [Huzita, 1980; Ishiwada and Ogawa, 1976]. Deformation

offshore would not, of course, be recorded by active faults on land. Thus, the recent increase in the rate of deformation in northeast Japan, implied by the difference in \dot{M}_0 obtained from the geologic and seismicity data, is probably not real but more likely reflects that the geologic record of fault offsets in northeast Japan is incomplete. Hence, \dot{M}_0 in northeast Japan is best constrained by the seismicity data.

In western Honshu, \dot{M}_0 computed from Quaternary fault data (2 to 9×10^{23} dyne cm/yr) is an order of magnitude less than \dot{M}_0 computed from the seismicity data (3.4×10^{24} dyne cm/yr). In western Honshu, seismic activity is about an order of magnitude less than seen in central Honshu, a region of approximately equal area. Thus, in western Japan a proportionately greater period of time ($>>400$ years) as compared to central Honshu is probably needed to obtain an accurate estimate of secular \dot{M}_0 from seismicity data. Hence \dot{M}_0 computed from the Quaternary fault data presents a better constraint for estimates of secular \dot{M}_0 . Geologically determined values of \dot{M}_0 (2 to 9×10^{23} dyne-cm/yr) convert to maximum rates of horizontal compressive strain and crustal shortening of 0.4 to 1.9×10^{-9} /yr and 0.1 to 0.7 mm/yr, respectively, oriented about 100° east of north.

In Shikoku, \dot{M}_0 estimated from the geologic data is about 5 to 7×10^{24} dyne cm/yr. Virtually all of this may be attributed to slip along the median tectonic line (MTL). The MTL has been aseismic for the last 1000 years [Matsuda, 1969, 1977] and does not show evidence of aseismic creep [Okada, 1970]. This suggests that enough energy is now stored along the MTL to produce an earthquake with seismic $M_0 = 5$ to 7×10^{27} dyne cm if strain buildup in this region has proceeded continuously through historic time [Shimazaki, 1976]. This is greater than the M_0 of the great 1891 Nobi earthquake. Figure 11b shows that the slip and orientation of the MTL are consistent with being caused by a compressive stress field that trends northwest.

Rates of deformation in the Izu Peninsula determined from seismicity data are median to the range of estimates obtained from fault data. The moment release and crustal shortening rates obtained with the fault data range from 2.1 to 11.8×10^{23} dyne cm/yr and 0.3 to 2.6 mm/yr, respectively (Table 5), in comparison to estimates of 4.4×10^{23} dyne cm/yr and 1.3 mm/yr assessed from the seismicity data (Figure 11a). The trend of maximum shortening indicated by each data set is also similar, trending about 30° west of north. The geologic data further show that the region immediately northward of the Izu Peninsula reflects similar rates of horizontal shortening (0.9 to 1.7 mm/yr) in a northerly direction (Figure 11b). The two data sets are thus consistent with the hypothesis that the rate and style of deformation in the Izu Peninsula has been relatively constant during the late Quaternary.

Discussion

The axes of maximum crustal shortening obtained from recent triangulation measurements [e.g., Nakane, 1973] show a pattern like that obtained in this study (Figure 11b). Geodetically measured rates of horizontal compressive strain

obtained by Nakane [1973], however, range up to 1 to 3 $\times 10^{-7}$ /yr as compared to 2 to 3 $\times 10^{-8}$ /yr determined in this paper. Similar observations have also been presented by Kaizuka and Imaizumi [1981]. We have measured only the permanent component of deformation as accommodated by slip on intraplate faults. The difference between our values and Nakane's [1973] must be attributed to other strain processes. Folding may account for part of the difference. Elastic compressive strain increase during the interseismic periods of great interplate earthquakes [e.g., Scholz and Kato, 1978; Shimazaki, 1974a, b; Yamashina et al., 1978] may also in large part produce the discrepancy in values measured by the two techniques. This component of strain, however, may not be considered permanent, since much of it may be released coseismically during the great interplate earthquakes [e.g., Scholz and Kato, 1978].

Strain release in Shikoku is predominantly taken up as slip along one major fault, the median tectonic line (MTL). The easterly strike of the MTL is consistent with a model in which oblique plate subduction of the Philippine Sea plate in a northwest direction is partially taken up by right-lateral motion along the MTL (Figure 3) [Fitch, 1972; Shimazaki, 1976]. Deformation of Honshu, in contrast, is distributed as slip on a system of many reverse and strike slip faults. The relative plate velocity vector between the Pacific and Eurasia, along the Japan trench, is about 9.7 cm/yr in an easterly azimuth (Figure 3). Maximum horizontal shortening in northeast Honshu, as accommodated by slip on intraplate faults, is also directed in an easterly direction and averages about 5 mm/yr. This suggests that about 5% of the relative plate velocity along the Japan trench is taken up as a relatively homogeneous compression of northeast Japan.

Interpretation of the intraplate stress field as being solely influenced by the transmission of compressive stress across the plate boundaries is, however, complicated by the observation that the central and western regions of Honshu are also characterized by an eastward compression rather than a northwestward compression, as might be expected from the proximity of the two regions to the Nankai trough. One must thus appeal to other factors in attempting to explain the east trending stress field of central and western Japan. The northward impingement of the Izu Peninsula into Honshu [Matsuda, 1978; Somerville, 1978] may affect the stress field in central Honshu similar to the way stresses in Asia are influenced by the continuing northward encroachment of India [Tapponnier and Molnar, 1977]. This is, however, quite speculative and a satisfying explanation of the stress field in central and western Japan remains a problem.

The major portion of the Japanese Islands was uplifted during the Quaternary period [Research Group for Quaternary Tectonic Map, 1973]. Similarly, the horizontal compressional tectonics of the Japanese Islands commenced at the onset of the Quaternary period (1-3 m.y. B.P.) [Sugimura, 1967]. This suggests that the two processes are physically related. Northeast Japan is characterized by reverse-type faulting. This geometry of faulting constrains horizontal shortening to be accompanied by vertical thickening. Our

analysis of the seismicity data in northeast Japan indicates that observed horizontal rates of shortening in northeast Japan should be accompanied by about 0.4 mm/yr thickening of the upper 15 km of the crust. Assuming that this is about 70% isostatically compensated, this thickening would result in only 0.1 to 0.2 mm/yr of observable uplift. In central Japan, virtually no uplift may be attributed to horizontal shortening of the seismogenic layer because faulting is predominantly strike slip. Quaternary (last 1 to 3 m.y.) uplift in northeast and central Japan is on average greater than 500 m. These observations thus indicate that processes responsible for most of the Quaternary uplift of the islands must be seated beneath the upper 15 km seismogenic layer. Strain thickening of the lithosphere beneath the seismogenic layer may play a significant role in the uplift process.

Conclusion

The seismicity and geologic data in Japan allow comparison of rates of seismic moment release and, hence, crustal shortening over time periods ranging from hundreds to greater than about 100,000 years. The rate of seismic moment release in intraplate Japan during the last 400 years has averaged 5 to 6 $\times 10^{25}$ dyne cm/yr. In central Japan, where seismic activity is predominantly located on land, the rate of seismic moment release calculated from recent seismicity data is in good agreement with the rate obtained from data describing the average slip rates of Quaternary faults. We interpret this result to suggest that the mode and rate of deformation we see in central Japan has been steady for at least the last 10,000 to 200,000 years. The seismicity and Quaternary fault data in the northeastern, western, and Izu Peninsula regions of intraplate Japan are also consistent with this hypothesis. Of direct consequence to the seismologist concerned with assessing seismic risk, the results obtained in this study further suggest that the release of seismic moment in intraplate Honshu is relatively free from secular variation when averaged over time periods of several hundreds of years.

Acknowledgments. The author (SGW) benefited greatly from conversations with several Japanese scientists when they visited the United States for the 1980 Ewing Symposium on Earthquake Prediction. In particular, T. Matsuda provided valuable discussions regarding the Quaternary geology of Japan; K. Ishibashi pointed out some new developments concerning the historical record of seismicity in Japan; and K. Yamashina kindly provided a copy of his doctoral thesis. I (SGW) would also like to thank Tom Hanks for suggesting that we use intensity data for estimating seismic moments of historical earthquakes and Larry Burdick, Art Frankel, Teruyuki Kato, Bill Menke, and Richard Quittmeyer for their constructive criticism. Edith Edsall provided assistance with seismology computing facilities. Word processing is by Erika Free. This paper was critically reviewed by Paul G. Richards and Terry Engelder. This research was supported by National Science Foundation grant CME-80-22096. Lamont-Doherty Geological Observatory contribution no. 3350.

References

- Abe, K., Fault parameters determined by near- and far-field data: The Wakasa Bay earthquake of March 26, 1963, Bull. Seismol. Soc. Am., 64, 1369-1382, 1974.
- Abe, K., Static and dynamic fault parameters of the Saitama earthquake of July 1, 1968, Tectonophysics, 27, 223-238, 1975a.
- Abe, K., Reexamination of the fault model for the Niigata earthquake of 1964, J. Phys. Earth, 23, 349-366, 1975b.
- Abe, K., Tectonic implications of the large Shioya-Oki earthquakes of 1938, Tectonophysics, 41, 269-289, 1977.
- Abe, K., Dislocations, source dimensions and stresses associated with earthquakes in the Izu Peninsula, Japan, J. Phys. Earth, 26, 253-274, 1978.
- Aki, K., Generation and propagation of G waves from the Niigata earthquake of June 16, 1964, parts I and II, Bull. Earthquake Res. Inst., Univ. Tokyo, 44, 23-88, 1966.
- Aki, K., and P. G. Richards, Quantitative Seismology: Theory and Methods, W. H. Freeman, San Francisco, Calif., 1980.
- Ando, M., Faulting in the Mikawa earthquake of 1945, Tectonophysics, 22, 173-186, 1974a.
- Ando, M., Seismotectonics of the 1923 Kanto earthquake, J. Phys. Earth, 22, 263-277, 1974b.
- Ando, M., Source mechanisms and tectonic significances of historical earthquakes along the Nankai trough, Japan, Tectonophysics, 27, 119-140, 1975.
- Brune, J. N., Seismic moment, seismicity, and rate of slip along major fault zones, J. Geophys. Res., 73, 777-784, 1968.
- Davies, G. F., and J. N. Brune, Regional and global fault rates from seismicity, Nature Phys. Sci., 229, 101-107, 1971.
- Fitch, T. J., Plate convergence, transcurrent faults, and internal deformation adjacent to southeast Asia and the western Pacific, J. Geophys. Res., 77, 4432-4460, 1972.
- Fitch, T. J., and C. H. Scholz, Mechanisms of underthrusting in southwest Japan: A model of convergent plate interactions, J. Geophys. Res., 76, 7260-7292, 1971.
- Fukao, Y., and M. Furumoto, Mechanisms of large earthquakes along the eastern margin of the Japan Sea, Tectonophysics, 25, 247-266, 1975.
- Gutenberg, B., and C. F. Richter, Seismicity of the Earth and Associated Phenomena, 310 pp., Princeton University Press, Princeton, N.J., 1954.
- Hagiwara, T., T. Yamamoto, T. Matsuda, and A. Daicho, Re-evaluation of the affected area of the 1614 Takada, Echigo earthquake (in Japanese), Programme Abstr. 1, pp. 39-40, Seismol. Soc. Jpn., Tokyo, 1980.
- Hanks, T. C., J. A. Hileman, and W. Thatcher, Seismic moments of the larger earthquakes of the southern California region, Geol. Soc. Am. Bull., 86, 1131-1139, 1975.
- Hasegawa, A., N. Umino, and A. Takagi, Double-planed structure of the deep seismic zone in the northeastern Japan arc, Tectonophysics, 47, 43-58, 1978.
- Hasegawa, T., S. Hori, A. Hasegawa, K. Kasahara, S. Horiuchi, and J. Koyama, On the mechanism of the earthquakes of southeastern part of Akita prefecture in 1970 (in Japanese with English abstract), J. Seismol. Soc. Jpn., 27, 302-312, 1974.
- Hatori, T., and M. Katayama, Tsunami behavior and source areas of historical tsunamis in the Japan Sea (in Japanese), Bull. Earthquake Res. Inst., Univ. Tokyo, 52, 49-70, 1977.
- Herrmann, R. B., S. Cheng, and O. W. Nuttli, Archeoseismology applied to the New Madrid earthquakes of 1811-1812, Bull. Seismol. Soc. Am., 68, 1751-1760, 1978.
- Honda, H., On the initial motion and the types of the seismograms of the North Izu and the Ito earthquakes, Geophys. Mag., 4, 185-213, 1931.
- Honda, H., On the mechanism and the types of the seismograms of shallow earthquakes, Geophys. Mag., 5, 69-88, 1932.
- Honda, H., and A. Masatsuka, On the mechanisms of the earthquakes and the stresses producing them in Japan and its vicinity, Sci. Rep. Tohoku Univ., Ser. 5, 4, 42-60, 1952.
- Honda, H., A. Masatsuka, and K. Emura, On the mechanisms of earthquakes and the stresses producing them in Japan and its vicinity (2nd paper), Sci. Rep. Tohoku Univ., Ser. 5, 8, 186-205, 1956.
- Honda, H., A. Masatsuka, and M. Ichikawa, On the mechanism of earthquakes and stresses producing them in Japan and its vicinity (3rd paper), Geophys. Mag., 33, 271-280, 1967.
- Huzita, K., Role of the median tectonic line in the Quaternary tectonics of the Japan Islands, Mem. Geol. Soc. Jpn., 18, 129-153, 1980.
- Ichikawa, M., Seismic activities at the junction of the Izu-Mariana and southwestern Honshu arcs, Geophys. Mag., 35(1), 55-69, 1970.
- Ichikawa, M., Reanalysis of mechanisms of earthquakes which occurred in and near Japan, and statistical studies on the nodal plane solutions obtained, 1926-1968, Geophys. Mag., 35(3), 207-274, 1971.
- Imamura, A., Topographic changes accompanying earthquakes or volcanic eruptions, Publ. 25, pp. 1-143, Earthquake Invest. Comm. Foreign Languages, Tokyo, 1930.
- Ishiwada, Y., and K. Ogawa, Petroleum geology of offshore areas around the Japanese Islands, Tech. Bull. U.N. Econ. Soc. Comm. Asia Pac., Comm. Co-ord. Jt. Prospect. Miner. Resourc. South Pac. Offshore Areas, 10, 23-34, 1976.
- Japan Meteorological Agency, Catalogue of major earthquakes which occurred in and near Japan (1926-1956), Seismol. Bull., Suppl. 1, pp. 1-91, Tokyo, 1958.
- Japan Meteorological Agency, Catalogue of major earthquakes in and near Japan (1957-1962), Seismol. Bull., Suppl. 2, pp. 1-49, Tokyo, 1966.
- Japan Meteorological Agency, Catalogue of major earthquakes in and near Japan (1963-1967), Seismol. Bull., Suppl. 3, pp. 1-62, Tokyo, 1968.
- Kaizuka, S., and Imaizumi, T., Horizontal strain rate of the Japanese Islands estimated from Active Fault Data (in Japanese), Programme Abstr. 1, p. 54, Seismol. Soc. Jpn., Tokyo, 1981.
- Kanamori, H., Focal mechanics of the Tokachi-Oki earthquake of May 16, 1968: Contortion of the lithosphere at a junction of two trenches, Tectonophysics, 12, 1-13, 1971.

- Kanamori, H., Tectonic implications of the 1944 Tonankai and the 1946 Nankaido earthquakes, Phys. Earth Planet. Inter., 5, 129-139, 1972.
- Kanamori, H., Mode of strain release associated with major earthquakes in Japan, Annu. Rev. Earth Planet. Sci., 1, 213-239, 1973.
- Kawasaki, I., The focal process of the Kita-Mino earthquake of August 19, 1961, and its relationship to a Quaternary fault, the Hatogayu-Koike fault, J. Phys. Earth, 24, 227-250, 1975.
- Kawasumi, H., Measures of earthquake danger and expectancy of maximum intensity throughout Japan as inferred from the seismic activity in historical times, Bull. Earthquake Res. Inst., Univ. Tokyo, 29, 469-482, 1951.
- Kayano, I., and Y. Sato, Distribution of seismic intensity of the Izu-Hanto-Oki earthquake of 1974, determined from questionnaires, Spec. Bull. Earthquake Res. Inst., Univ. Tokyo, 14, 7-16, 1974.
- Kikuchi, B. D., Recent Seismological Investigations in Japan, 120 pp., Tokyo Printing Co., Ltd., Tokyo, 1904.
- Kostrov, B. V., Seismic moment and energy of earthquakes, and seismic flow of rock, Izv. Acad. Sci. USSR Phys. Solid Earth, 1, 23-40, 1974.
- Maki, T., On the earthquake mechanism of the Izu-Hanto-Oki earthquakes of 1974, Spec. Bull. Earthquake Res. Inst., Univ. Tokyo, 14, 23-36, 1974.
- Matsuda, T., Active faults and large earthquakes (in Japanese), Kagaku Tokyo, 39, 398-407, 1969.
- Matsuda, T., Surface faults associated with Nobi (Mino-Owari) earthquake of 1891, Japan, Spec. Bull. Earthquake Res. Inst., Univ. Tokyo, 13, 85-126, 1974.
- Matsuda, T., Empirical rules on sense and rate of recent crustal movements, J. Geod. Soc. Jpn., 22, 252-263, 1976.
- Matsuda, T., Estimation of future destructive earthquakes from active faults on land in Japan, J. Phys. Earth, Suppl., 25, S251-S260, 1977.
- Matsuda, T., Collision of the Izu-Bonin arc with central Honshu: Cenozoic tectonics of the Fossa Magna, Japan, J. Phys. Earth, Suppl., 26, S409-S421, 1978.
- Matsuda, T., S. Kaizuka, Y. Ota, T. Imaizuma, Y. Ikeda, S. Hirano, and M. Togo, Preliminary report on the trench across the Tanna fault, Izu, Japan (in Japanese), Chiri Tokyo, 26, (6), 122-129, 1981.
- Mikumo, T., Faulting mechanism of the Gifu earthquake of Sept. 9, 1969, and some related problems, J. Phys. Earth, 21, 191-212, 1973.
- Mikumo, T., Some considerations on the faulting mechanism of the southeastern Akita earthquake of October 16, 1970, J. Phys. Earth, 22, 87-108, 1974.
- Mikumo, T., and M. Ando, A search into the faulting mechanism of the 1891 great Nobi earthquake, J. Phys. Earth, 24, 63-87, 1976.
- Murai, I., A report on damage and seismic intensity by the Kawazu earthquake in 1976, Bull. Earthquake Res. Inst., Univ. Tokyo, 52, 2, 1977.
- Murai, I., N. Tsunoda, and Y. Tsujimura, Damage, seismic intensities, and earthquake faults by the Izu-Oshima-Kinkai earthquake of 1978, Bull. Earthquake Res. Inst., Univ. Tokyo, 53, 3, 1978.
- Nakamura, K., and S. Uyeda, Stress gradient in arc-back arc regions and plate subduction, J. Geophys. Res., 85(B11), 6419-6428, 1980.
- Nakane, K., Horizontal tectonic strain in Japan (I and II) (in Japanese with English abstract), J. Geod. Soc. Jpn., 19, 190-208, 1973.
- Nishimura, K., Characteristic features of focal mechanisms in and near Kyushu Island (1), Contrib. Geophys. Inst., Kyoto Univ., 13, 101-110, 1973.
- Oida, T., and K. Ito, Foreshock-aftershock sequence of the earthquake off the Atsumi Peninsula on Jan. 5, 1971 (in Japanese with English abstract), J. Seismol. Soc. Japan, 25, 178-186, 1972.
- Oike, K., On a list of hypocenters compiled by the Tottori Microearthquake Observatory (in Japanese with English abstract), J. Seismol. Soc. Jpn., 28, 331-346, 1975.
- Okada, A., Fault topography and rate of faulting along the median tectonic line in the drainage basin of the river Yoshino, northeastern Shikoku (in Japanese), Jpn. Geogr. Rev., 43, 1-21, 1970.
- Omori, F., Notes on the Earthquake Investigation Committee Catalogue of Japanese earthquakes, J. Coll. Sci. Imp. Univ. Tokyo, 11, 389-436, 1899.
- Research Group for Active Faults of Japan, Active faults in Japan, sheet maps and inventories, Univ. of Tokyo Press, Tokyo, 1980a.
- Research Group for Active Faults of Japan, Active faults in and around Japan: The distribution and the degree of activity, J. Nat. Disaster Sci., 2(2), 61-99, 1980b.
- Research Group for Quaternary Tectonic Map, Explanatory text of the Quaternary tectonic map of Japan, Natl. Res. Cent. for Disaster Prevention, Sci. and Tech. Agency, Tokyo, March 1973.
- Richter, C. F., Elementary Seismology, W. H. Freeman, San Francisco, Calif., 1958.
- Scholz, C. H., and T. Kato, The behavior of a convergent plate boundary: Crustal deformation in the South Kanto District, Japan, J. Geophys. Res., 83, 783-797, 1978.
- Seno, T., The instantaneous rotation vector of the Philippine Sea plate relative to the Eurasian plate, Tectonophysics, 42, 209-226, 1977.
- Shimazaki, K., Pre-seismic crustal deformation caused by an underthrusting oceanic plate in eastern Hokkaido, Japan, Phys. Earth Planet. Inter., 8, 148-157, 1974a.
- Shimazaki, K., Nemuro-Oki earthquake of June 17, 1973: A lithospheric rebound at the upper half of the interface, Phys. Earth Planet. Inter., 9, 314-327, 1974b.
- Shimazaki, K., Intraplate seismicity gap along the median tectonic line and oblique plate convergence in southwest Japan, Tectonophysics, 31, 139-156, 1976.
- Shimazaki, K., and P. Somerville, Static and dynamic parameters of the Izu-Oshima, Japan, earthquake of Jan. 14, 1978, Bull. Seismol. Soc. Am., 69, 1343-1378, 1979.
- Shimazaki, K., T. Kato, and K. Yamashina, Basic type of internal deformation of the continental plate at arc-arc junctions, J. Phys. Earth, Suppl., 26, Suppl. S69-S83, 1978.
- Shiono, K., Travel time analysis of relatively deep earthquakes in southwest Japan with

- special reference to the underthrusting of the Philippine Sea plate, J. Geosci. Osaka City Univ., 18(4), 37-59, 1974.
- Shiono, K., Focal mechanisms of major earthquakes in southwest Japan and their tectonic significance, J. Phys. Earth, 25, 1-26, 1977.
- Shiono, K., and T. Mikumo, Tectonic implications of subcrustal normal faulting earthquakes in the western Shikoku region, Japan, J. Phys. Earth, 23, 257-278, 1975.
- Somerville, P., The accommodation of plate collision by deformation in the Izu block, Japan, Bull. Earthquake Res. Inst., Univ. Tokyo, 53, 3, 1978.
- Sugimura, A., Uniform rates and duration period of Quaternary earth movements in Japan, J. Geosci. Osaka City Univ., 10, 1-4, 1967.
- Takagi, A., A. Hasegawa, and N. Umino, Seismic activity in the northeastern Japan arc, J. Phys. Earth, 25, 595, 1977.
- Takeo, M., K. Abe, and H. Tsuji, Mechanism of the Shizuoka earthquake of July 11, 1935 (in Japanese with English abstract), J. Seismol. Soc. Jpn., 32, 423-434, 1979.
- Tapponnier, P., and P. Molnar, Active faulting and tectonics in China, J. Geophys. Res., 82, 2905-2930, 1977.
- Thatcher, W., T. Matsuda, T. Kato, and J. B. Rundle, Lithospheric loading by the 1896 Rikuu earthquake in northern Japan: Implications for plate flexure and asthenospheric rheology, J. Geophys. Res., 85, 6429-6435, 1980.
- Trifunac, M. D., and A. G. Brady, On the correlation of seismic intensity scales with the peaks of recorded strong ground motion, Bull. Seismol. Soc. Am., 65, 139-162, 1975.
- Usami, T., Descriptive table of major earthquakes in and near Japan which were accompanied by damages (in Japanese with English abstract), Bull. Earthquake Res. Inst., Univ. Tokyo, 44, 1571-1622, 1966.
- Usami, T., Descriptive Catalogue of Disaster Earthquakes in Japan (in Japanese), 327 pp., Univ. Tokyo Press, Tokyo, 1975.
- Usami, T., and O. Hamamatsu, History of earthquakes and seismicity (in Japanese): In Y. Sato (Ed.), Seismology in Japan, J. Seismol. Soc. Jpn., Ser. 2, 20(4), 1-34, 1967.
- Utsu, T., Seismicity of Japan from 1885 through 1925--A new catalogue of earthquakes of $M < 6$ felt in Japan and smaller earthquakes which caused damage in Japan (in Japanese with English abstract), Bull. Earthquake Res. Inst., Univ. Tokyo, 54, 223-308, 1979.
- Watanabe, K., N. Hirano, and Y. Kishimoto, Seismicity in the Hokurika District (in Japanese with English abstract), J. Seismol. Soc. Japan, 31, 35-47, 1978.
- Yamashina, K., Focal mechanisms of earthquakes in Japan and their possible contributions to the following seismic and volcanic activities, Ph.D. thesis, 264 pp., Univ. of Tokyo, Tokyo, 1976.
- Yamashina, K., and I. Murai, On the focal mechanisms of the earthquakes in the Oita prefecture and in the northern part of Aso of 1975, especially the relations to the active fault system (in Japanese with English abstract), Bull. Earthquake Res. Inst., Univ. Tokyo, 50, 295-302, 1975.
- Yamashina, K., K. Shimazaki, and T. Kato, Aseismic belt along the frontal arc and plate subduction in Japan, J. Phys. Earth, Suppl., 26, S447-S458, 1978.
- Yoshii, T., Proposal of the 'aseismic front' (in Japanese), J. Seismol. Soc. Jpn., 28, 365-367, 1975.

(Received October 20, 1981;
revised May 3, 1982;
accepted May 14, 1982).